

Review

# A Review on Emerging Cementitious Materials, Reactivity Evaluation and Treatment Methods

Ashfaque Ahmed Jhatial <sup>\*</sup>, Iveta Nováková  and Eirik Gjerløw 

Department of Building, Energy and Material Technology, The Arctic University of Norway, Lodve Langes gata 2, 8514 Narvik, Norway

\* Correspondence: ashfaque.a.jhatial@uit.no

**Abstract:** Alternative to traditional concrete, sustainable concrete reduces cement content, waste management issues, and CO<sub>2</sub> emissions. To achieve sustainable concrete, waste materials can be used as supplementary cementitious materials (SCMs) to partially replace cement. Fly ash, ground-granulated blast furnace slag, and silica fume have been heavily studied as SCMs. However, due to the retirement of coal-fired power plants and switching to renewable energy, existing SCMs are losing their dominance. With SCMs becoming more widely accepted as partial cement substitutes, there is fear that the current supply will not meet future demand. As a result, researchers have been looking for alternative SCMs. The circular economy can be achieved by reusing non-hazardous construction and demolition materials, timber, and metal/steel production waste as SCMs. This article discusses emerging SCMs, reactivity evaluation methods, their limitations, and treatment methods that may improve reactivity. Emerging SCMs can replace existing SCMs in quantity, but their supply to cement factories and low reactivity due to stable crystallinity hinders their use. Among treatment methods, particle size reduction effectively enhances reactivity; however, very fine SCM may increase the overall water demand due to the large surface area. Decades-old reactivity evaluation methods have relatively weak correlations and thus misreport the reactivity of SCMs. Newer R<sup>3</sup> models, such as calorimetry and bound water, give the best correlations ( $R \geq 0.85$ ) for 28-day relative strength and better performance. Additionally, more concrete testing with emerging SCMs under different durability and environmental protection conditions is required and life cycle assessments are needed to determine their regional environmental impact.



**Citation:** Jhatial, A.A.; Nováková, I.; Gjerløw, E. A Review on Emerging Cementitious Materials, Reactivity Evaluation and Treatment Methods. *Buildings* **2023**, *13*, 526. <https://doi.org/10.3390/buildings13020526>

Academic Editor: Flavio Stochino

Received: 11 January 2023

Revised: 7 February 2023

Accepted: 10 February 2023

Published: 15 February 2023



**Copyright:** © 2023 by the authors. Licensee MDPI, Basel, Switzerland. This article is an open access article distributed under the terms and conditions of the Creative Commons Attribution (CC BY) license (<https://creativecommons.org/licenses/by/4.0/>).

**Keywords:** sustainable concrete recycling; supplementary cementitious materials (SCMs); environmental hazards; natural resources conservation; reactivity testing; treatment methods

## 1. Introduction

As a result of the availability of raw materials (cement, fine and coarse aggregates, water, and admixtures), flexibility in shape and size, and durability when subjected to varying environmental conditions, concrete has become the most popular building and construction material in the world. However, the widespread use of concrete harms the environment and human health because of the significant amount of greenhouse gases released during manufacturing. The cement industry, the product of which is the sole binder material for concrete, is one of the most energy-intensive industries [1]. According to CEMBUREAU [2], 667 kg CO<sub>2</sub>eq per metric tonne of cement was the European average in 2017. High CO<sub>2</sub> emissions are generated during mining and transportation of raw materials to the cement factory, during cement manufacture, in the batching plant, and distribution.

Between 1930 and 2013, it has been estimated that approximately 76.2 billion tonnes of cement were produced, which resulted in the release of 38.2 billion tonnes of CO<sub>2</sub> [3]. The contribution of the cement industry to total global CO<sub>2</sub> gas emissions varies, ranging from 5% to 10%; however, the cement industry's CO<sub>2</sub> emissions have had a substantial effect on the surrounding ecosystem. CO<sub>2</sub> is a powerful greenhouse gas that contributes to global

warming by absorbing and radiating heat, keeping the planet warm more than any other greenhouse gas. The increase in greenhouse gases has disrupted the Earth's energy budget, resulting in a higher average temperature worldwide. The rise in global construction activity drives up demand for cement, and as that demand grows, so does the amount of CO<sub>2</sub> produced by cement manufacture. The rising energy costs for ordinary Portland cement (OPC) production are linked to CO<sub>2</sub> emissions. Though cement production and demand have increased exponentially over the years, the industry is starting to face challenges such as depleting natural resources, rising energy costs, and needing to reduce CO<sub>2</sub> emissions to meet sustainability goals; thus, finding solutions is unavoidable. Increasing energy efficiency or using alternative materials can reduce the environmental impact of concrete [4]. The United Nations Environmental Program's Sustainable Building and Climate Initiative recommended clinker replacement [5]. According to Yang et al. [6], the carbon footprint can be reduced by using biofuels or low-carbon fuels during clinker milling, improving the CO<sub>2</sub> capture mechanisms, migrating from wet to dry clinker production, and using supplementary cementitious materials (SCMs) to partially substitute clinker content. Of the four mitigating methods, using SCMs is probably the most cost-effective and practical remedial measure [7] being utilized worldwide.

### 1.1. Supplementary Cementitious Materials (SCMs)

SCMs are inorganic materials that contribute to concrete's properties. SCMs can be either inert, latent hydraulic, or pozzolanic [1]. Inert SCMs act as filler materials, functioning as a nucleation site that helps speed up cement's hydration and hardening process while also filling pores and favoring microstructural densification in cement-based products. Latent hydraulic SCMs (rich calcium or reactive silicates) will react with water to form calcium-silicate hydrate (C-S-H) gels with or without OPC [8]. During the reaction, the dissolution of silica in water forms silicic acid (H<sub>4</sub>SiO<sub>4</sub>) [9], which then consumes Ca(OH)<sub>2</sub> to form C-S-H gels [10,11]. The pozzolanic reaction occurs when pozzolans (siliceous [12], or siliceous aluminous [13] materials that do not possess cementitious properties themselves) come into contact with cement and consume Ca(OH)<sub>2</sub> produced during hydration, thus forming C-S-H gels and densifying the microstructure.

According to Habert et al. [14], cement represents only roughly 10% of concrete's mass but it accounts for 74–80% of the total CO<sub>2</sub> emissions of concrete [15]. By substituting portions of the cement used in concrete with SCMs, it is possible to reduce the CO<sub>2</sub> emissions per unit of concrete. Studies have shown that if large parts of the construction industry adopted the use of SCMs, the CO<sub>2</sub> emissions from using cement could be reduced by up to 20% [15]. As SCMs are often by-products or waste products of various industrial processes, the CO<sub>2</sub> emissions attributed to them are much lower than those of cement. Most of the emissions from SCMs are due to preparation and are commonly so low that they are overlooked. SCMs produced from waste materials also have the added environmental benefit of reducing the amount of waste going into landfills.

### 1.2. Standardized SCMs

Using SCMs has been one of the most effective methods to reduce negative environmental impacts during cement production. Additionally, the concrete industry can improve the efficiency of concrete mixture designs (e.g., increasing strength-to-mass ratios) and the longevity of concrete structures, thus reducing associated emissions with the SCMs [16]. As mentioned earlier, SCMs can be classified as either inert (such as limestone powder, quartz, and marble powder), latent hydraulic (ground granulated blast furnace slags and basic oxygen furnace slags), and pozzolanic. Pozzolanic SCMs are further divided into (1) artificial pozzolans and (2) natural pozzolans. Artificial pozzolans, such as fly ash and silica fume, are industrial by-products. Natural pozzolans are usually abundant in silica, aluminum, and iron. They can be further classified into two types: natural rocks such as volcanic glass and pumicite, which may require to be mechanically treated before being utilized, and soils such as calcined clays and metakaolin, which may require thermal

treatment for activation. Natural pozzolans have been used in construction for thousands of years, with the most famous example being the use of volcanic tuffs and pumice by the Romans in their constructions. Natural pozzolans have large accessible reserves and are easy to treat; however, they have high water demand. In this section, we describe the materials that are well-established and utilized as SCMs: coal fly ash, ground granulated blast furnace slag, silica fume, and limestone powder.

### 1.2.1. Fly Ash

Fly ash (FA), the most-used SCM, was coined in the 1930s but Carlson et al. [17] first used it in 1937. The Hungry Horse Dam in the United States of America, built in 1948, was the first structure to use FA in the concrete mix [17]. In 1980, global ash production surpassed 200 million tons, with 14% used in concrete [17]. In 1989, 561 tonnes were produced, with 16% used in concrete [17]. Since 1977, the use of FA in concrete has tripled. According to recent reports, approximately 12.6 million tonnes of FA were used in 2018 [18].

FA is a powdery by-product of pulverized coal combustion [19,20]. FA (which accounts for 80%), bottom ash, slags, and flue gas desulfurization products are coal combustion by-products [21]. Coal-fired power plants produce around 750 million tonnes annually [22]. FA's vast applications include extracting metals and making zeolites, adsorbents, geopolymers, and ceramics [23]. FA can be siliceous or calcareous depending upon the coal type, and it primarily contains solid spheres and hollow cenospheres containing crystalline materials and unburnt carbon [24]. FA is used in cement and concrete because of its fineness, chemical and phase composition, and pozzolanic activity. FA consists of  $\text{SiO}_2$ ,  $\text{Al}_2\text{O}_3$ ,  $\text{Fe}_2\text{O}_3$ , and  $\text{CaO}$ , with smaller amounts of  $\text{MgO}$ ,  $\text{Na}_2\text{O}$ ,  $\text{K}_2\text{O}$ ,  $\text{SO}_3$ ,  $\text{MnO}$ ,  $\text{TiO}_2$ , and unburnt carbon. Loss on ignition (LOI) depends on the type of power plant and working regime and can range from 1% to 10%. ASTM C618 [25] and European EN 450-1 [26] classify and regulate FA's chemical and physical properties. ASTM C618 classifies FA by LOI and  $\text{SiO}_2$ ,  $\text{Al}_2\text{O}_3$ , and  $\text{Fe}_2\text{O}_3$  content. Pozzolan is the sum of  $\text{SiO}_2$ ,  $\text{Al}_2\text{O}_3$ , and  $\text{Fe}_2\text{O}_3$ . Meanwhile, EN 450-1 classifies FA by LOI and reactive silica content. Figure 1 illustrates the influence of FA content on the compressive strength and carbonation depth, compared to other SCMs.

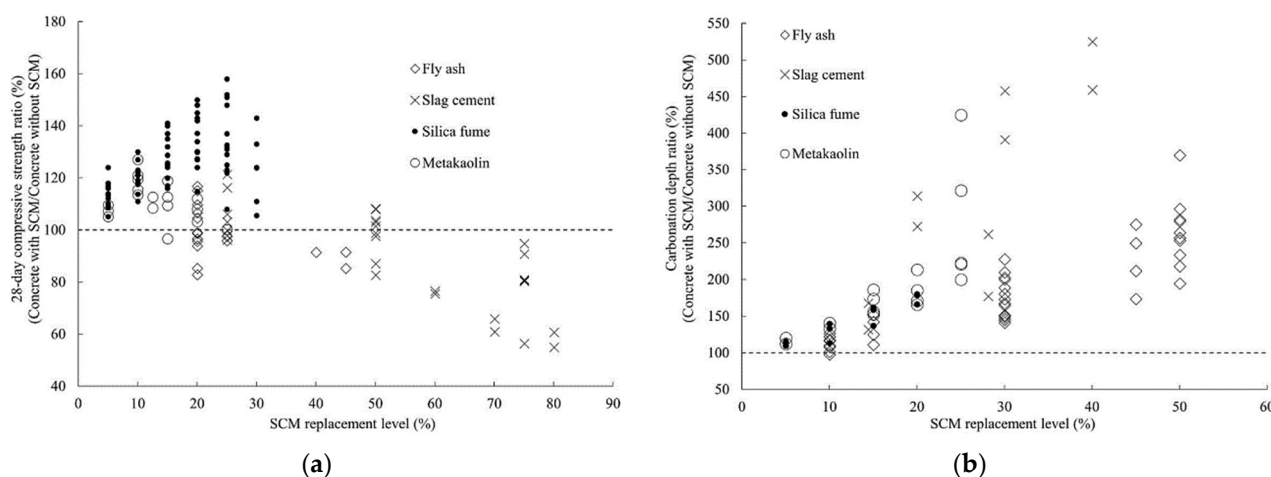


**Figure 1.** Influence of SCM replacement level on (a) compressive strength (b) carbonation depth of concrete [27].

Johri et al. [28] found that FA increases concrete workability while reducing water demand. FA-replaced concrete had low early strength due to dilution and slow pozzolanic reactions. Concrete with 10–30% FA content (cement replacement) showed 1–5% lower strength at 28 days compared to the control sample. At 180 and 365 days, concrete with 10–30% FA had higher compressive strength than the control sample, with concrete containing 30% FA showing an 11.54% increase. Behl et al. [29] also found that 5–20% FA increased the compressive strength of concrete. As shown in Figure 1, the compressive strength decreases with the increase in FA content; however, the effect of FA on the carbonation depth is lower

compared to other SCMs. At the same time, 30% and 40% FA in high-strength concrete reduced sorptivity, chloride ion permeation, and drying shrinkage, according to Nath and Sarker [30]. Similar findings were also observed by Saha [31] when FA class F was used. The reduction in sorptivity was attributed to the high specific surface area of FA, which limited the interfacial transition zone (ITZ). The decrease in chloride permeability was attributed to alkali binding and low interconnecting voids. Islam [32] also noted that concrete containing FA exhibited better freeze-thaw resistance due to the formation of secondary C-S-H gels during the pozzolanic reaction of FA, which filled voids and reduced the corrosion of embedded steel reinforcements.

### 1.2.2. Ground Granular Blast Furnace Slag

Ground granulated blast furnace slag (GGBS) is a by-product of steel and iron production. By-products such as slags are unavoidably produced during iron and steel production [33]. Langen discovered GGBS's latent hydraulic reactivity in the early 1860s in Germany, and Germany began commercially producing slag-lime cement in 1865 [34]. "Eisenportlandzement" was first manufactured in 1901 and consisted of 30% GGBS, while "Hochofenzement" was produced in 1907 and increased the GGBS content to 85% [34]. The World Steel Association [35] estimated the steel production of 2020 at 1878 million tonnes. Approximately 300 kg GGBS is generated per ton of pig iron, while 100–150 kg GGBS is generated per ton of molten steel [36]. The global GGBS production is estimated to be 300–360 million tonnes [37]. GGBS mainly contains 28–41% SiO<sub>2</sub>, 37–50% CaO, and 5–14% Al<sub>2</sub>O<sub>3</sub> [38]. GGBS is a latent hydraulic material with cementitious properties, despite containing pozzolanic oxides. Over the years, like FA, GGBS has been widely used in the construction industry.

Increasing GGBS content increases workability. According to Johari et al. [28], 20% GGBS achieved 9.19% higher compressive strength than control concrete; however, a further increase in GGBS content significantly reduced the strength gain. Boukendakdji et al. [39] found that 20% GGBS improved the workability of self-compacting concrete but reduced its strength. Kuo et al. [40] found that when GGBS replacement was 0–30%, the compressive strength ranged from 11.6 to 5.3 MPa on Day 1, 24.4 to 21.4 MPa on Day 7, and 31.7 to 29.1 MPa on Day 28. Adding 30% GGBS increased the mix's flow value by 28 mm compared to the control sample. Onn et al. [41] used up to 70% GGBS as SCM in mortar and found a reduction in compressive strength. Zhou et al. [42] reported a slight decrease in the 28-day compressive strength of 30% GGBS concrete [24]. Similarly, Gholampour and Ozbakkaloglu [43] found 50% GGBS reduced concrete strength by 9% after 7 days and 6% after 28 days. A similar trend can be seen in Figure 1. Though GGBS has self-cementing properties, the reduction in strength has been attributed to the slow rate of hydration and lower amount of hydration products [41]. Bheel et al. [44] used GGBS along with metakaolin in a binary blend and found that even with metakaolin, the workability decreased compared to the reference concrete; however, 5% GGBS and 5% metakaolin exhibited enhancements in compressive, tensile, and flexural strengths after curing for 28 days and carbonation and chloride penetration decreased. Aghaeipour and Madhkhan [45] found that adding GGBS increased the moisture content of roller-compacted concrete, allowing for maximum compaction. Concrete with 40% GGBS had reduced porosity, water absorption, and permeability. However, freeze-thaw cycles caused significant deterioration due to specimen saturation.

### 1.2.3. Limestone Powder

Limestone powder (LP), the powdery by-product of a limestone quarry, is made by crushing and grinding natural limestone and consists of calcite, aragonite, vaterite, and amorphous calcium carbonate [46]. OPC contains fine limestone. Early literature called limestone "inert filler" [47]. It is the main component in most masonry cement, where high Portland cement replacement is needed to replicate traditional lime mortar [47]. When co-ground with clinker, limestone can significantly contribute to hydration reactions in con-

crete [47]. It may be used as an SCM along with GGBS and FA. Several European countries used LP in Portland cement during WWII to cut costs and boost output. France led the 1973 oil crisis despite low FA and GGBS production [47]. Portland cement manufacturers in the US have changed the formulation of their most important product to reduce embodied carbon by approx. 10% by adding LP [48,49].

Table 1 shows the chemical composition of LP, also known as calcium carbonate ( $\text{CaCO}_3$ ) [46]. The chemical composition of LP depends on the source of the raw material, since limestone formation, minerals, processing, and refinement affect the composition. The availability and cost-effectiveness of LP compared to other SCMs, such as FA and GGBS, have allowed it to be used as an SCM [50]. Table 1 shows that LP does not contain significant pozzolanic oxides, so no pozzolanic reactions occur and no C-S-H gels are developed [51]. Recent studies have shown that LP is not an inert filler, as there is little interaction between tricalcium silicate ( $\text{C}_3\text{S}$ ) and  $\text{CaCO}_3$  [52]. The  $\text{C}_3\text{A}\cdot\text{CaCO}_3\cdot 11\text{H}_2\text{O}$  and  $\text{C}_3\text{A}\cdot 3\text{CaCO}_3\cdot 32\text{H}_2\text{O}$  hydration phases are only obtained with 400–600 °C steam-cured concrete [53]. Adding LP as an SCM in concrete can trigger filler, nucleation, dilution, and chemical effects, thus accelerating hydration, precipitating C-S-H, and changing the particle surface morphology [46].

**Table 1.** Chemical composition of LP (Note: Sum \* is the sum of pozzolanic oxides).

Sample	SiO <sub>2</sub>	Al <sub>2</sub> O <sub>3</sub>	Fe <sub>2</sub> O <sub>3</sub>	Sum *	CaO	K <sub>2</sub> O	MgO	SO <sub>3</sub>	Na <sub>2</sub> O	TiO <sub>2</sub>	LOI	Ref
1	0.20	-	0.15	0.35	55.11	0.02	1.12	0.09	-	-	43.31	[50]
2	0.86	0.08	0.31	1.25	56.3	0.05	0.58	-	0.08	-	42.0	[54]
3	0.84	0.24	0.32	1.4	53.96	0.34	1.01	-	-	-	43.01	[55]
4	8.97	1.02	0.37	10.36	46.77	0.13	2.38	0.33	0.02	-	39.54	[56]

Nepomuceno et al. [57] found that 20–60% LP in cement improved cohesion and restricted segregation. Wang et al. [58] observed that LP reacted with cement at a low rate even after 5 years. Lin et al. [59] investigated the influence of 10%, 20%, and 30% LP on mortar's mechanical properties and durability. It was noticed that the inclusion of LP decreased the permeability and durability while increasing the mechanical strength. The compressive and splitting tensile strengths increased with the addition of LP. However, the magnitude of strength gain decreased with increased LP content. With 10% LP, mortar or concrete was stronger than with the reference mix [58,59]. In addition, it was observed that the addition of LP decreased the permeability of concrete, which may negatively influence its durability. However, Wang et al. [58] found that the compressive strength of concrete containing 10% LP remained almost constant with a small fluctuation from 1 to 5 years, whereas that with the reference mix gradually increased. This could be attributed to the concrete's hydration, which reached its maximum extent after one year. It could also be due to the limited hydration products generated from the reaction between LP and cement, thus have very little impact on the overall long-term strength.

Increased LP content hinders the formation of hydration products needed to fill capillary and gel pores, resulting in lower density [59]. When the LP content increased, the total charge passed increased during chloride penetration due to an increase in fine pores [59]. Wang et al. [58] observed that the reference concrete's chloride permeability was higher than that of the concrete with LP at 28 days; however, all concrete with and without LP showed a significant drop in charge passed. At 5 years, the reference concrete and 10% LP concrete had low permeability, while the 20% and 30% LP concretes had moderate permeability. Wang et al. [58] reported that an LP content above 10% reduced concrete's carbonation resistance and dry shrinkage. Kim et al. [51] found that 10% LP concrete had a similar drying shrinkage curve, while increasing the LP content reduced dry shrinkage, agreeing with the results of Wang et al. [58]. The pore structure deteriorated with more than 25% LP.

#### 1.2.4. Silica Fume

Silica fume (SF) is a by-product of smelting silicon and ferrosilicon in an electric arc furnace [27]. Smelting reduces high-purity quartz to silicon, producing SiO<sub>2</sub> vapors that oxidize and condense into micro non-crystalline silica particles. Table 2 shows that non-crystalline silica particles contain 85% silica. The composition of silica fume can vary due to differences in the source material, manufacturing process, and impurities present. Variation in silica content is associated with alloy type; for example, SF generated during ferrosilicon alloy production has lower silica content and reduced pozzolanic activity. SF, as an SCM, is newer than FA and GGBS. First used as an additive in Norway in the 1950s, SF gave good concrete strength, durability, and sulfate resistance [60]. SF could not be used until the late 1960s or early 1970s after the Norwegian government announced environmental legislation involving huge improvements in filtering technology [60].

**Table 2.** Chemical composition of SF (Note: Sum \* is the sum of pozzolanic oxides).

Sample	SiO <sub>2</sub>	Al <sub>2</sub> O <sub>3</sub>	Fe <sub>2</sub> O <sub>3</sub>	Sum *	CaO	K <sub>2</sub> O	MgO	SO <sub>3</sub>	Na <sub>2</sub> O	TiO <sub>2</sub>	LOI	Ref
1	92.50	0.70	1.56	94.76	0.60	1.17	0.80	0.24	0.36	-	2.07	[61]
2	90.2	0.24	2.4	92.84	0.65	1.26	0.41	0.4	0.16	0.02	3.33	[62]
3	96.57	0.06	0.06	96.69	0.51	0.73	0.25	0.17	0.16	0.01	1.41	[63]
4	95.3	0.65	0.28	96.23	0.27	-	0.41	0.25	0.76	-	-	[64]

SF nanoparticles (0.1 to 0.3 μm) are 100 times smaller than cement particles [65]. SF particles are spherical, while the color varies from greyish-black powder to premium white. The fineness and silica content allow SF to have effective pozzolanic activity. SF is known in the construction industry worldwide for its ability to improve concrete's pore refinement, abrasion resistance, bond strength, permeability, and early strength. Table 3 summarizes findings for SF-containing concrete/mortar. Mechanical strength also increased with the addition of SF, suggesting no dilution effect or that its substitution changed the performance [66]. SF improves the ITZ, thus increasing compressive strength [67] and freeze-thaw durability [68]. Likewise, Lu et al. [69] found that strength increased by 38% when 16% SF was used.

**Table 3.** Effect of SF on flow and strength properties of cement composites.

SF Content (by wt. of Cement)	Difference Compared to Control Mix (%)			
	Workability	Compressive	Splitting Tensile	Flexural
5%	↓ 14.67% [70] ↓ 20.25% [71]	↑ 21.5% [66], ↑ 15.29% [70], ↑ 7.81% [72], ↑ 1.59% [73], ↑ 23.04% [74]	↑ 6.45% [70], ↑ 47.75% [72] ↑ 5.04% [73]	↑ 21.06% [72], ↑ 2.06% [75], ↑ 4.49% [74]
10%	↓ 26.67% [70] ↓ 29.11% [71]	↑ 36.9% [66], ↑ 27.45% [70], ↑ 22.09% [72], ↑ 5.34% [73] ↑ 20.99% [74]	↑ 11.29% [70], ↑ 54.82% [72], ↑ 27.95% [73]	↑ 54.11% [72], ↑ 5.91% [75], ↑ 12.36% [74]
15%	↓ 33.33% [70] ↓ 49.37% [71]	↑ 7.84% [70], ↑ 23.50% [72], ↓ 16.01% [73]	↑ 3.23% [70], ↑ 65.95% [72], ↓ 2.76% [73]	↑ 60.62% [72] ↑ 3.08% [75],
20%	↓ 54.43% [71]	↓ 15.59% [72], ↓ 24.08% [73]	↓ 29.34% [72], ↓ 12.36% [73]	↑ 21.40% [72], ↑ 5.41% [76] ↑ 0.51% [75]

Apart from the increased workability of the mix, the combination of SF with other SCMs, such as FA [77,78], GGBS [74], copper slag [79], nano-silica [80] and metakaolin [64,77] increased the strength and durability of concrete due to accelerated hydration, differential reactions, and the dilution effect caused by the different SCMs. In some rare cases, the addition of SF increased the workability of the mix; for example, Mohyidden and Maya [81] observed that concrete containing copper slag had reduced workability but the workability increased with the addition of SF along with copper slag. Padavala et al. [82] observed a similar trend when SF was used in combination with FA.

### 1.3. Industrial Application of Standardized SCMs

Binary (one cement, one SCM) or ternary (one cement, two SCMs) blends of SCMs with cement are increasingly used in industry due to their improved concrete properties and lower cement content. Existing SCMs, such as FA, SF, LP, and GGBS, have been extensively evaluated over the past few decades. Table 4 illustrates the volumes of existing SCMs being used. Their benefits have been recognized and adopted by the cement and concrete industries [83].

**Table 4.** Estimated yield and utilization volume (million tonnes per year) of standardized SCMs [16].

SCM	Chemistry	Estimated Volume	Utilized	Remarks
Coal Fly Ash (FA)	Si-Al	700–1100	330–400	Lower pozzolanic reactivity, carbon content
Ground Granulated Blast Furnace Slag (GGBS)	Ca-Si-Al	300–360	330	Latent hydraulic reactivity, fully used
Silica fume (SF)	Si	1–2.5	0.5–1	Preferred in high performance concrete
Limestone (LP)	CaCO <sub>3</sub>	Large accessible reserves	300	Cementitious contribution in combination with reactive aluminates
Calcined Clays	Si-Al		3	Metakaolin being used, high water demand
Natural Pozzolans	Si-Al		75	High water demand, large variability

Currently, the availability of existing SCMs can only satisfy 15% of the demand of the concrete industry [84], with FA being the dominant SCM [38]; however, the decommissioning of coal-fired power plants and switch to renewable energy sources has eroded its dominance. Eliminating coal as an energy source is crucial to meeting the Paris Agreement's 1.5 °C target [85]. Many countries plan to phase out coal-fired power plants by 2030, which will affect the FA supply [85]. The GGBS supply is dwindling due to increased steel recycling and direct iron reduction [86]. SF is expensive, so using it instead of cement may increase production costs. Existing SCMs are not produced or available everywhere, so some regions must transport them long distances, thereby increasing CO<sub>2</sub> emissions and cost. New alternatives, such as calcinated clay or natural pozzolans, are soon to be or already standardized (LC3 and Heidelberg cement/Norcem Newcem—basaltic glass from Iceland). Cement demand could reach 6 billion tonnes by 2050 [87]. The industry is rapidly evolving with increased international trade of SCMs; thus, the exploration of new SCM resources is crucial.

## 2. Emerging SCMs

A vast pool of by-products and wastes from industrial, agricultural, and municipal processes can become new SCMs. Presently these by-products and wastes cause waste management issues, and their further reuse might be slightly more challenging thanks to their varying chemical or physical character. Nevertheless, these materials can partially replace cement in cementitious composites, thus reducing cost and pollution. This article reviews selected waste materials and evaluates their potential of becoming new SCMs. As most materials suitable for SCM have undergone different processes and operations, they

may lack the required reactivity; therefore, different methods to evaluate and enhance the potential SCM's reactivity are revisited.

### 2.1. Mine Tailings

Mine tailings are the residual solid waste generated during mining and mineral processing operations from the different mechanical and chemical processes involved. Mine tailings can be fine-grained slurries made of milled minerals, gravel, or process water [88]. Globally, 3240 million tonnes of metallic mineral ores were mined, and iron ore mining contributed 93.5% [89]. As the quantity of mined minerals is large, so is the quantity of tailings [90]. One tonne of iron, copper ore, and bauxite generates 1.5, 1, and 1.5 tonnes of tailings, respectively. The chemical composition of tailings depends on the mined metal and source rock, as shown in Table 5. The low pozzolanic reactivity of mine tailings depends on the minerals' reactivity or the stable crystalline structure [91]. Low pozzolanicity prevents the use of mine tailings as an SCM.

**Table 5.** Chemical composition of various mine tailings.

Tailings Type	CaO	SiO <sub>2</sub>	Al <sub>2</sub> O <sub>3</sub>	Fe <sub>2</sub> O <sub>3</sub>	MgO	K <sub>2</sub> O	SO <sub>3</sub>	P <sub>2</sub> O <sub>5</sub>	Na <sub>2</sub> O	LOI	Ref
Bauxite	3.15	32.24	37.39	8.67	0.85	-	-	-	-	13.74	[92]
Copper	0.16–2.90	60.90–79.52	7.66–17.03	3.60–4.22	0.49–1.53	1.85–2.63	1.11–4.50	0.34	0.11–4.30	2.10–4.26	[93,94]
Gold	1.06–13.60	35.50–72.86	6.80–13.68	1.11–9.70	0.08–5.90	0.50–5.32	0.16–0.70	-	<0.70–3.04	1.40–12.90	[95–97]
Iron	0.09–13.68	33.26–56.00	7.92–10.96	8.30–50.96	0.43–6.50	0.18–2.31	0.01–10.59	0.18–0.31	1.72	3.30–9.60	[98–100]
Phosphate	36.80	2.10	0.10	0.80	18.90	-	1.00	-	0.10	35.80	[101]
Quartz-based	0.51	79.53	9.52	3.22	0.64	3.24	-	-	0.72	2.46	[102]
Zn-Pb	13.60–20.01	35.50–43.26	6.80–11.11	6.40–15.57	4.00–4.31	1.00–4.10	0.32–2.00	-	<0.70–0.92	5.10–5.61	[96,103]

Table 5 shows that most tailings, except phosphate tailings, exhibit potential pozzolanic properties. The mine tailings' physical properties, as shown in Table 6, are less erratic than the chemical oxides. The particle sizes can be classified into three categories: sand, silt, and clay. Mine tailings have a rougher and more irregular surface [104] owing to varying mineral grinding. Grinding and mineral phases affect the density and water absorption of mine tailings. Due to advances in grinding, mine tailings contain more silt and clay, and even if used as an aggregate, their maximum size is less than 1 mm [105].

**Table 6.** Physical properties of various mine tailings (Note: + indicates the skeletal density through helium pycnometer while \* indicates the relative density).

Tailing	Specific Gravity	Blaine Specific Surface Area (cm <sup>2</sup> /g)	Density (g/cm <sup>3</sup> )	Water Absorption (%)	Ref
Gold	3.46	368	-	7.15	[106]
Iron	2.60–3.53	553.8–735	1.27*–3.67 <sup>+</sup>	7.00	[98,99,107]
Copper	2.75–4.29	537–5776	-	13.82	[108,109]

Tailings have a rough, irregular surface, high crystallinity, and particle size that is incompatible with the hydration of cement [110], and even though they are rich in silicon, they cannot be utilized as an SCM for concrete because of their low reactivity. Previous studies [94,111] have reported the reduced performance of concrete containing tailings as an SCM. To enhance their reactivity, mine tailings can be treated using mechanochemical and thermal methods [112]. The mine tailings are first air-dried to remove any moisture content

and then passed through a 600  $\mu\text{m}$  sieve in order to remove any impurities [112]. Meanwhile, other researchers [113] suggested that the tailings should only pass through a 45  $\mu\text{m}$  sieve. Wang et al. [97] produced OPC clinker using gold mine tailings (GT) as a substitute for natural sandstone. The burnability analysis indicated that the GT had high reactivity. The clinker phases  $\text{C}_3\text{S}$ ,  $\text{C}_2\text{S}$ ,  $\text{C}_3\text{A}$ , and  $\text{C}_4\text{AF}$  and feldspar and mica were detected, suggesting that adding GT to cement clinker raw materials could reduce the bauxite content. GT did not affect the consistency or the setting times of the cement. Its compressive and flexural strengths were 59.1 and 9.8 MPa on 28-day testing, respectively, which were slightly higher than those of the control specimens, while flaky  $\text{Ca}(\text{OH})_2$ , rod-shaped ettringite, and granular C-S-H gel hydration products were observed. Similar clinker phases were observed by Wang et al. [114] when GT was added to cement clinker. X-ray diffraction (XRD) analysis indicated that the hydration products of cement with GT were identical to those observed for cement without GT. The lack of detection of any diffraction peaks for C-S-H was attributed to the poor crystallization and amorphous properties of the C-S-H gels [97,114]. Based on Table 7, it was observed that the addition of 5% GT achieved the highest strength while further addition of GT caused a significant decrease in strength.

**Table 7.** Influence of mine tailings on Portland cement clinker.

Mine Tailing	Raw Material Proportions of Clinker (%)	Consistency (%)	Setting Time (min)		Compressive Strength (MPa)			Flexural Strength (MPa)			Ref
			Initial	Final	3 Days	7 Days	28 Days	3 Days	7 Days	28 Days	
GT	85.79% LS, 6.28% B, 2.53% ICM, 5.41% SS	24.5	140	212	28.3	43.8	57.7	5.8	7.2	9.5	[97]
	85.36% LS, 3.79% B, 3.29% ICM, 7.56% GT	24.8	138	215	30.4	44.7	59.1	6.1	7.6	9.8	
IOT	77.08% LS, 17.65% C, 1.38% QS, 3.89% IO	23.0	165	225	20.7	-	46.2	4.9	-	8.5	[115]
	75.07% LS, 6.31% QS, 1.31% IO, 17.31% IOT	23.8	160	235	20.8	-	48.6	4.9	-	8.5	
IOT	0% Clay substitution	-	136	190	21.2	-	50.6	-	-	-	[116]
	IOT as 10% clay substitution	-	132	185	24.1	-	52.3	-	-	-	
	IOT as 20% clay substitution	-	105	142	16.6	-	38.4	-	-	-	

Note: For this table, LS = limestone, SS = sandstone, C = clay, B = bauxite, ICM = iron corrective material, QS = quartz sand, IO = iron ore, GT = gold tailing, IOT = iron ore tailings.

De Magalhães et al. [117] prepared mortar specimens incorporating 10%, 20%, and 30% IOT. Compressive strengths of 41.65, 36.26, and 31.64 MPa were determined for the 10%, 20%, and 30% IOT-based mortars, respectively, which were significantly lower than that of the control sample. The loss in strength was attributed to the low pozzolanic activity of IOT caused by the low specific surface area and percentage of amorphous phase in the IOT. In another study, in which De Magalhães et al. [118] utilized heat-treated IOT at 500 and 750  $^{\circ}\text{C}$  as cement replacement, it was observed that the particle grain size of IOT was smaller than that of cement. The heat treatment eliminated the presence of kaolinite minerals that may have transformed into an amorphous phase, thus transforming IOT into pozzolan and changing its color. Zinc mine tailings (ZMT) consist of quartz, dolomite, and aluminum element phases. Agrawal et al. [119] utilized treated (mechanically) and untreated zinc mine tailings (ZMT) to substitute 5%, 10%, 15%, and 20% cement content. Although the chemical composition of ZMT indicated that it was a class C pozzolan, only the concrete with 5% treated and untreated ZMT achieved mechanical properties comparable to the control sample. It was observed that the sample with untreated

zinc consisted of larger-sized particles with a less rough surface than control cement particles. The addition of ZMT did not affect the concrete's quality. Nevertheless, it was reported that the water absorption rate and carbonation depth of the ZMT-based concrete samples increased with the increase in substitution level. The rise in carbonation depth and water absorption was attributed to less dense structures and increased pore volume and size observed in concrete when ZMT was utilized. This assertion was also confirmed by the findings of Wang et al. [114] using IOT. Earlier studies on different mine tailings indicated that the workability decreased with the increase in the substitution level due to the increased specific area of the tailings. Though most mine tailings are pozzolanic, they have low pozzolanic reactivity, and thus negatively affect the mechanical properties of concrete. Some mechanically treated tailings do not increase pozzolanic reactivity as much as calcination due to the high kaolinite content.

## 2.2. Slags from Metal Production

There are number of different slags generated during metal production. GGBS has been the frontline slag thanks to being volumetrically stable and can be straightforwardly used in the construction industry. In contrast, other slags have high pH due to free (unhydrated) CaO causing volumetric instability (expansion) [120,121]. Each specific slag must undergo proper slag aging, testing, and quality control, and thoroughly evaluated for the intended purpose to ensure that the slag can potentially be of use in construction. Therefore, research has been ongoing and focused on slags for construction applications.

### 2.2.1. Aluminum Dross

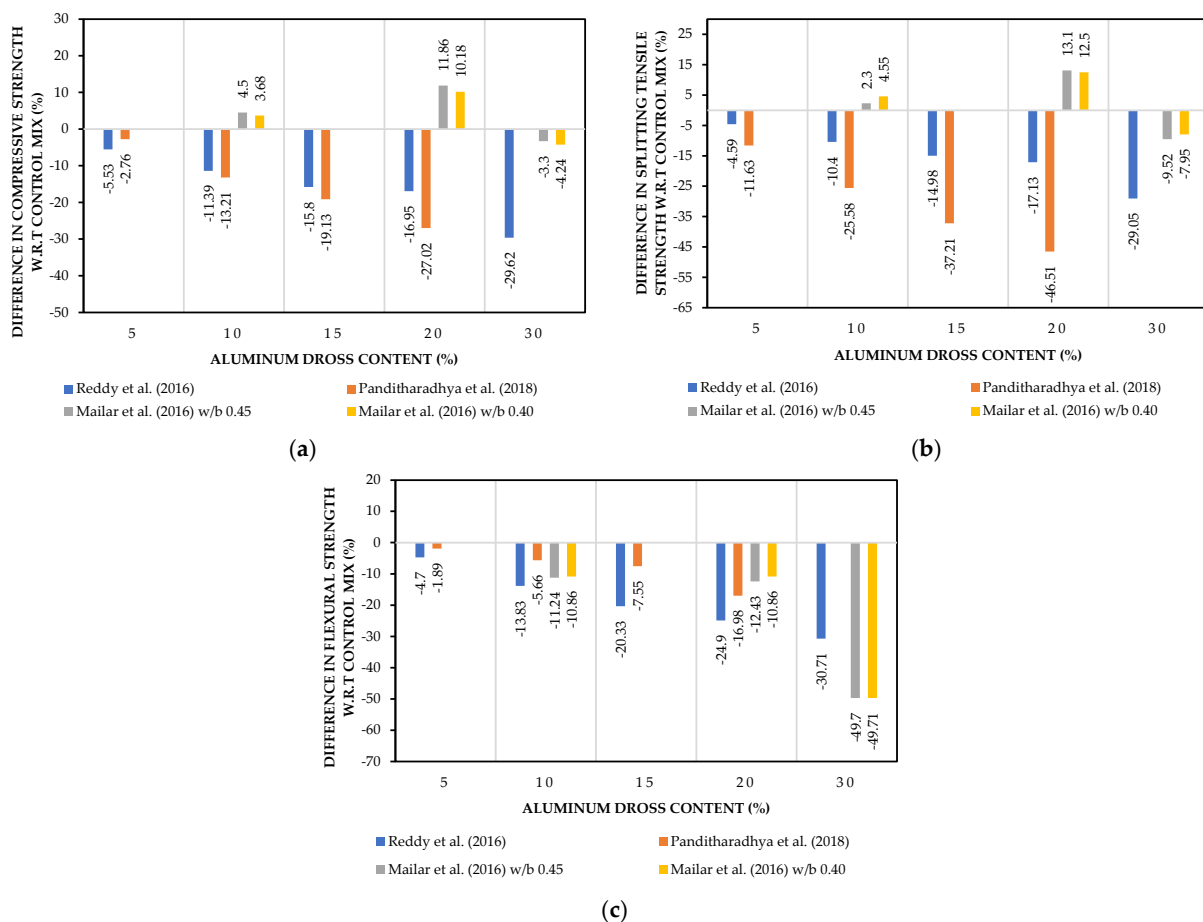
Aluminum dross (AD) is a by-product of aluminum smelting [122]. A salt cake is produced from this procedure that is currently dumped in landfills [122]. The composition of recycled AD varies depending on the factory that produces it [123]. AD comprises aluminum, alumina, aluminum nitride, salts, and other oxides [124]. This complicated composition makes it challenging to reutilize. AD can be categorized into two types, namely (1) primary aluminum dross, which is a solid form with high aluminum content (more than 50% of the total weight of dross), and (2) secondary aluminum dross, which is granular in shape and has low aluminum content (5 to 20%) [125]. Regenerated AD contains harmful elements and its disposal is not eco-friendly. The Environmental Protection Agency [126] says dross is a highly flammable, non-corrosive material that can cause skin inflammation, leaching, and health and environmental issues. Four million tonnes of primary aluminum dross and one million tonnes of secondary aluminum dross are produced annually [127]. Almost all AD is landfilled near factories, but rain can lead to toxic metal ions penetrating surface and ground water, causing ecological issues [125]. Table 8 lists AD's chemical and mineral composition, which can vary by raw material or metallurgical process [125]. Rapid chemical screening indicates that AD is pozzolanic, according to ASTM C618 [25], and the sum of  $\text{SiO}_2 + \text{Al}_2\text{O}_3 + \text{Fe}_2\text{O}_3$  is significantly higher than 70%. AD has been used to make cement mortar, bricks, lightweight expanded clay aggregates, calcined alumina, and refractory clay. Additionally, AD has also been used as a cementitious material and limited data showed that 20% AD improved the strength and permeability of concrete [122,128,129].

Table 8. Chemical composition of AD.

$\text{Al}_2\text{O}_3$	$\text{SiO}_2$	$\text{Fe}_2\text{O}_3$	$\text{AlCl}_3$	$\text{FeSO}_3$	$\text{CaO}$	$\text{SO}_3$	$\text{Ca}(\text{FeO}_3)$	$\text{Al}(\text{OH})_3$	$\text{MgO}$	$\text{AlN}$	$\text{LOI}$	Ref
79.68	4.14	-	0.52	0.68	4.25	-	6.95	2.18	-	0.1	0.05	[130]
63.29	6.36	0.32	-	-	20.2	6.36	-	-	0.45	-	5.3	[122]
77.15	1.34	1.02	-	-	0.56	-	-	-	1.86	8.06	-	[127]
63.84	7.15	0.03	-	-	0.07	0.03	-	-	0.04	-	-	[131]

Reddy et al. [131] replaced cement with 5–30% secondary AD, and it was observed that increasing the AD content increased the normal consistency to 40%. The initial and final setting times increased, which was attributed to the presence of silicates. The AD reduced the concrete compressive strength by 5.53% to 29.62%, with tensile and flexural strengths following a similar

trend. The reduction in strength was attributed to the dilution effect caused by the decrease in clinker content and increased AD content, resulting in less  $\text{Ca}(\text{OH})_2$  consumed by the AD during pozzolanic reactivity and fewer hydration products. However, the mechanical properties and durability significantly improved when up to 15% AD was utilized, along with up to 15% SF and 30% FA. Panditharadhy et al. [132] evaluated using 5–20% secondary AD in concrete. The initial and final setting followed a similar trend reported by Reddy et al. [131], as shown in Table 9. Figure 2 illustrates the variations in the mechanical strength of concrete when different AD contents are utilized. It was observed that the mechanical strength decreased with the increase in AD content. However, 5% AD showed a minor strength loss compared to the control concrete, and 15% AD was considered optimum as it achieved the minimum target strength required for M40 grade concrete according to IS-10262-2009 for India (equivalent to C40/50 according to EN 206-1). Javali et al. [130] also observed that 5% AD concrete achieved almost identical strengths as the control concrete. Concrete with 5% AD along with 10%, 20%, 30%, and 40% iron slag as a fine aggregate replacement demonstrated improved concrete properties, with 5% AD plus 20% iron slag achieving almost similar strength as the control concrete. The pozzolanic and filler effect of AD and iron slag, respectively, were attributed to the enhancement in the properties [130]. However, according to the findings of Mailar et al. [122], it can be observed that the addition of AD in concrete gives significantly better compressive and tensile strengths but reduced flexural strength, which has been attributed to the inhomogeneity in the distribution of hydration products in hot weather conditions. Furthermore, Mailar et al. [122] observed that AD concrete exhibited 20–30% more resistance to acid attack, while the water absorption was reported to be significantly lower than that of control concrete, thus indicating that AD improves the durability of concrete.



**Figure 2.** Variation in (a) compressive strength, (b) splitting tensile strength and (c) flexural strength of concrete incorporating different aluminum dross contents (data from ref. Mailar et al. [122], Reddy et al. [131] and Panditharadhy et al. [132]).

**Table 9.** Influence of AD on the properties of concrete.

% Of AD		0	5	10	15	20	30	0	5	10	15	20
Consistency (%)		34	34	34	34	38	40	30	31	32	34	38
Setting Time (min)	Initial	40	45	55	65	80	90	50	55	65	80	95
	Final	380	270	240	220	200	180	390	360	310	290	220
Ref				[131]				[132]				

In short, AD has significant potential to be used as an SCM after different treatments or blending with other SCMs [130].

### 2.2.2. Iron and Steelmaking Slags

The worldwide iron and steel output has rapidly increased in recent years [133]. A considerable amount of slag is always formed during the steel production process. The sector predicts an upward tendency in future output and slag quantity [133]. Usually, iron and steelmaking slags can be categorized as GGBS, basic oxygen furnace (BOF) slag, electric arc furnace (EAF) slag, or ladle furnace (LF) slag, according to the considered production process [134].

For every ton of crude steel produced in a BOF, approximately 100–150 kg of slag is generated as waste [135]. From 2000 to 2018, pig iron production climbed from 575.78 to 1252.87 million tonnes, steel from BOF increased from 522.68 to 1282.54 million tonnes, and steel from EAF rose from 287.26 to 523.92 million tonnes [133]. In terms of utilization in concrete, GGBS has been widely used and, according to some research, can substitute 80% of cement [136]. However, other slags could be used as different ingredients in concrete production based on their physical properties (Table 10) and chemical composition (Table 11). Rapid screening indicated that the sum of  $\text{SiO}_2 + \text{Al}_2\text{O}_3 + \text{Fe}_2\text{O}_3$  was slightly below 50% for GGBS, BOF, and LF slags, thus they could not be considered as a pozzolanic materials but were latent hydraulic materials. EAF slag could be considered a pozzolanic material since the sum of pozzolanic oxides is 57.62% and amorphous phases are present [137,138]. However, different treatment methods, such as particle size reduction, thermal treatment, and additives (as explained in Section 3), enhance the quality and fineness of slags, thus increasing their pozzolanic activity. Based on their properties, metal slags can be used as cementitious material. Table 12 illustrates the results using different slags.

**Table 10.** Physical properties of different metal slags.

Slag	Dimensions (mm)	Density ( $\text{kg/m}^3$ )	Surface Area ( $\text{cm}^2/\text{g}$ )	Water Absorption (%)	Ref
GGBS	$\leq 0.063$	2810–2910	4250–4620	2.1	[139–141]
BOF	0.018	2690–3480	4515	0.4	[142,143]
EAF	0.013–0.063	2840–3337	4990	4.32	[139,142,144]
LF	0.063	1540	-	2	[139,145]

**Table 11.** Chemical composition of different metal slags (Note: Sum \* is the sum of pozzolanic oxides) (adopted from ref. [133]).

Slag	$\text{SiO}_2$	$\text{Fe}_2\text{O}_3$	$\text{Al}_2\text{O}_3$	Sum *	CaO	MgO	MnO	$\text{SO}_3$	$\text{TiO}_2$	$\text{P}_2\text{O}_5$	$\text{Na}_2\text{O}$	$\text{K}_2\text{O}$	$\text{Cr}_2\text{O}_3$	ZnO
GGBS	34.03	0.74	11.39	46.16	38.26	8.65	0.92	0.62	3.58	-	-	-	-	-
BOF	13.59	25.73	3.59	42.91	42.59	7.91	2.77	0.4	1.71	1.32	-	-	0.02	-
EAF	16.23	33.05	8.34	57.62	27.71	5.21	4.57	0.13	0.7	1.76	0.13	0.1	2.57	0.44
LF	20.86	1.75	10.95	33.56	53.29	7.18	2.76	1.25	0.29	0.1	1.16	0.22	0.45	-

**Table 12.** Influence of slags on the compressive strength (MPa).

Slag	% of Cement Replaced										Ref
	Control	1%	3%	5%	10%	15%	20%	25%	30%	35%	
BOF	31.5 ± 0.4	32.1 ± 0.3	38.5 ± 0.2	42.2 ± 0.2	40.6 ± 0.1	36.1 ± 0.5	-	-	-	-	[146]
	39.57	-	-	-	-	37.93	-	-	-	-	[141]
EAF	53.6	-	-	-	48.1 ± 3.7	-	44.75 ± 1.75	-	44.95 ± 0.95	-	[147]
	66.5	-	-	-	-	64.6	-	-	51.4	-	[148]
LF	59.34	-	-	-	-	-	43.06 ± 5.36	-	-	-	[139]

As shown in Table 12, 15% EAF slag had a slight reduction of 2.86% compared to the control mix [137]. In other studies conducted by Roslan et al. [148] and Roslan et al. [149], in which 5%, 10%, 15%, and 20% EAF slag was used, it was observed that 10% EAF slag achieved higher 28-day compressive strength than the control mix. It was further observed that all mixes with EAF slag achieved slightly higher compressive strength after curing for 90 days, suggesting that EAF slag was a pozzolanic material since the concrete gained further strength as it cured. Jexembayeva et al. [146] obtained the highest compressive strength with 5% BOF slag compared to the control mix, which was also reported by Shi et al. [150], who used superfine steel slag in cement mortar. Fine microparticles of BOF slag accelerated hydraulic reactivity, boosting early and late strengths. A higher BOF slag content decreased the compressive strength compared to the control mix. It has been found that the slag source affects the concrete's properties. EAF slag reduces concrete strength, but it can achieve similar strengths as the control mix if ground into superfine particles. Parron-Rubio et al. [139] found an 11 MPa difference in strength between the two types of LF slags, but the strength was significantly lower when 25% LF slag was used from both sources. LF slag's reactivity as an SCM can be enhanced so that the concrete gains more strength using the treatment methods mentioned in Section 3; however, the most effective method to improve the reactivity of LF slag is mechanical reduction of particle size since this increases surface area contact, developing more nucleation sites for chemical reactions.

### 2.3. Wood Waste Ash

Increased timber production and interest in renewable energy will increase the use of wood waste as fuel in thermal power plants, resulting in vast amounts of wood ash. The combustion of wood waste generates a lot of ash and residue compounds, which can cause health and ecological problems [151]. This residue ash is commonly known as wood waste ash (WWA) or biomass ash. WWA can be divided into bottom ash and fly ash based on the combustion technology or how the ashes are contained [152]. Wood bottom ash is coarser than wood fly ash. One ton of wood waste as fuel produces 5 MWh of energy and 50 kg of ash [153]. The typical disposal of WWA is in landfills, which accounts for 70% of WWA, while 20% of WWA is utilized as a soil fertilizer, and the remainder is used for other purposes. Different power plants use different combustion technologies, methods, and fuels, which affect WWA's physical properties and heavy metal concentration. The presence of heavy metals in WWA may cause groundwater contamination due to rainwater leaching or seepage. When ash reacts with water, the pH rises, reducing the solubility of heavy metals and other trace elements. The alkalinity of ash changes when it dissolves in an acidic environment like forest soil, thus exposing the metals to a pH far lower than that of ash and increasing their solubility.

WWA's potential use depends on its chemical and physical properties, which vary by location, tree species, incineration method, and temperature. WWA particles are irregular,

spherical, and highly porous [154,155]. Some WWA has crystal-like spikes, which increase the surface area and porosity [152]. The chemical composition, to some extent, reflects the reactivity of WWA and the incineration conditions. Uncontrolled incineration may lead to high alkalinity and pH, which could range from 9 to 13.5 [156].

As observed from Table 13, the chemical composition vastly varies for WWA depending on the source, and WWA can either have pozzolanic or latent hydraulic potential.

**Table 13.** Chemical composition of various wood ash from various timber sources (Note: Sum \* is the sum of pozzolanic oxides) [151,157].

Wood Waste Ash	CaO	SiO <sub>2</sub>	Al <sub>2</sub> O <sub>3</sub>	Fe <sub>2</sub> O <sub>3</sub>	Sum *	K <sub>2</sub> O	MgO	P <sub>2</sub> O <sub>5</sub>	SO <sub>3</sub>	Na <sub>2</sub> O	TiO <sub>2</sub>
Forest Residue	47.55	20.65	2.99	1.42	25.06	10.23	7.2	5.05	2.91	1.6	0.4
Pine Dark	56.83	9.2	7.2	2.79	19.19	7.78	6.19	5.02	2.83	1.97	0.19
Poplar Bark	77.31	1.86	0.62	0.74	3.22	8.93	2.36	2.48	0.74	4.84	0.12
Sawdust	44.11	26.17	4.53	1.82	32.52	10.83	5.34	2.27	2.05	2.48	0.4
Spruce Bark	72.39	6.13	0.68	1.9	8.71	7.22	4.97	2.69	1.88	2.02	0.12
Wood Residue	11.66	53.15	12.64	6.24	72.03	4.85	3.06	1.37	1.99	4.47	0.57

Awolusi et al. [158] used 2.5% and 5% sawdust-based WWA (obtained by uncontrolled burning) in concrete, observing that the water absorption decreased up to 4.62% compared to 4.93% exhibited by the control sample. Furthermore, higher silica and ash contents increased the water demand and reduced the workability. Raza et al. [159] investigated the influence of 5% to 20% WWA at increments of 5% on the properties of concrete. It was found that WWA reduced the workability of fresh concrete (reductions of 9.59% to 97.26%), water absorption (reductions of 10.80% to 45.15%), and density (reductions of 1.43% to 4.96%). It was further observed that 20% WWA in concrete achieved a 45% decrease in water absorption compared to the control concrete. With the utilization of 5% and 10% WWA, the concrete achieved strengths of 32.61 and 32.6 MPa (14.58% and 14.55% increases) respectively, compared to 28.46 MPa achieved by the control mix. The pozzolanic reactivity of WWA allowed the concrete to gain strength; however, beyond 10% WWA, the concrete strength significantly declined, such that approximately 22.79% strength was lost with 20% WWA. This was attributed to the excess silica content that could not be fully reacted, thus WWA acted as a filler material instead of a binder material. Bhat [160] varied the water-cement ratio (0.42, 0.45, and 0.50) while using 10–20% WWA in self-compacting concrete. The author observed that WWA concrete required more superplasticizer to be as workable as the control concrete, while the compressive and splitting tensile strengths were also reduced irrespective of the water-cement ratio.

## 2.4. Waste from Concrete Production Activities

### 2.4.1. Concrete Sludge

Concrete sludge waste (CSW) is waste from ready-mix or precast concrete plants [161]. Figure 3 shows how wastewater from ready-mix trucks and batching plants is transferred to sedimentation tanks where fine materials settle, known as CSW. The amount of CSW generated globally is difficult to quantify; however, based on the total global production of 4 billion tonnes of cement [162], it can be estimated that CSW production is around 260 million tonnes [161]. In Europe, fresh concrete waste generated during manufacture or truck cleaning/washing is estimated to be 1–4% of the total concrete produced [163]. This CSW is challenging to handle and has a high pH, making it hazardous to the environment and human health. Due to its high alkalinity (pH > 11.5), CSW is considered corrosive in the UK, Spain, and the USA [164], and improperly dumped CSW may damage the environment and ecosystem.

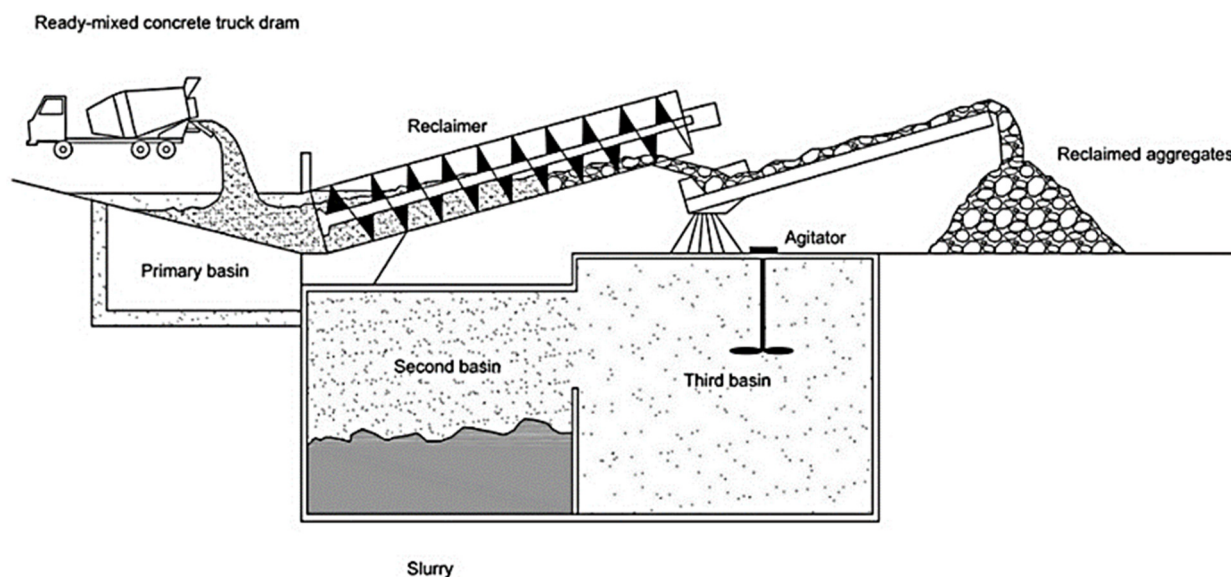


Figure 3. Illustration of CSW and reclaimed concrete aggregates [165].

CSW is composed of cement's hydrated/carbonated residuals and the finest portion of aggregates. Due to its high water content, CSW is considered workable only for a few days. Once it dries, the color becomes dull grey and can quickly be ground into fine powder. The specific gravity can range between 2.3 to 2.5, the specific surface area can be 4300 to 18,000 cm<sup>2</sup>/g, while the Blaine fineness ranges from 7540 to 9940 cm<sup>2</sup>/g [166]. CSW contains hydration products (up to 70%), while fine aggregates have a significant presence (30%). CSW particles have an angular shape. The CaCO<sub>3</sub> and Ca(OH)<sub>2</sub> contents can total up to 49% [150], while the pH can be up to 13. From Table 14, it can be observed that SiO<sub>2</sub> and CaO are the two main components of CSW. At the same time, the LOI is high due to the decomposition of CaCO<sub>3</sub> and C-S-H [163] and may also be attributed to the natural carbonation of fine particles when exposed to the atmosphere.

Table 14. Comparison of chemical compositions of CSW with OPC. (Note: Sum \* is the sum of pozzolanic oxides).

Material	SiO <sub>2</sub>	CaO	Al <sub>2</sub> O <sub>3</sub>	Fe <sub>2</sub> O <sub>3</sub>	Sum *	K <sub>2</sub> O	Na <sub>2</sub> O	TiO <sub>2</sub>	MgO	P <sub>2</sub> O <sub>5</sub>	SO <sub>3</sub>	LOI	Ref
OPC	19.57	64.51	3.81	3.12	26.5	0.69	-	0.27	1.48	-	5.43	1.08	[167]
CSW	32.84	36.92	8.21	6.72	47.77	1.6	-	0.54	1.88	-	2.81	8.58	[167]
CSW	28	36	9.4	7	44.4	1.5	1	-	1.6	0.3	3.7	10.7	[161]
CSW	17.7	44.4	5.1	3.1	25.9	0.3	-	0.5	1.5	-	2.2	14.2	[168]
CSW	36.49	20.58	14.35	4.34	55.18	1.73	0.35	-	2.67	-	1.22	17.13	[169]

Based on the literature [167], four methods have been identified for the management of CSW, namely (1) landfilling, (2) producing SCM by grinding and sieving processes, (3) producing recycled fine/coarse aggregates, and (4) using fresh CSW as a cementitious paste. Currently, the most common strategy is landfill disposal [170], which involves dewatering of CSW such that the grey wash water is removed and dry solid CSW is transported to landfills [167]. Although it may be the most used, the strategy is not an environmentally sustainable approach as the process involves energy and fuel consumption and emissions.

In a previous study [171] using 0.5 to 400 µm grain-sized calcareous CSW to replace 10–30% cement, it was found that CSW had a low salt content, while the XRD analysis revealed calcite and traces of dicalcium silicate (C<sub>2</sub>S) peaks, indicating that it was fully hydrated. With the increase in CSW content, an increase in superplasticizer was required

to achieve the same workability as the control specimen. Concrete with 10% CSW achieved similar compressive strength development, while that with 20% CSW exhibited 5.5% lower compressive strength compared to the control mix. It has been observed that the filler effect caused by CSW incorporation affects the binder's pH. The pH significantly affects the hydration; however, the adverse effect on the compressive strength was mitigated using CSW with high alkalinity (pH of 12.1). Loss in flexural strength was also observed with the increase in CSW content, which was attributed to the deterioration of the ITZ. According to the findings of Ferriz-Papi [172], dried but unground CSW cannot be used for cement substitution because the reduction in compressive strength was significant compared to the reference mortar. Further, it was observed that the increase in CSW content decreased the compressive strength, such that approximately 30% strength loss was obtained with 25% CSW compared to the control mix.

Keppert et al. [161] utilized fresh, dewatered, and reclaimed CSW, observing that 10% of the CSW was unhydrated clinker residuals (alite, belite, brownmillerite), aluminate phases, and small traces of hydrotalcite, suggesting the concrete was slag-based cement. It was observed that 10% CSW did not adversely influence the strength of the concrete owing to its high fineness (2 to 200  $\mu\text{m}$ , with an average particle size of 7  $\mu\text{m}$ ), which imposed a higher water content, but an increase in CSW content resulted in a loss in strength. Similar findings were also observed by Xi et al. [171]. However, the high water demand could be mitigated with water-reducing admixtures. It was also determined that concrete incorporating CSW had a high chloride binding capacity, which could be potentially beneficial where steel reinforcements need to be protected from degrading environmental mechanisms. The study demonstrated that fresh CSW could be utilized on-site.

#### 2.4.2. Recycled Concrete Powder (RCP)

Although RCP consists of portions of hydrated and unhydrated cement and accounts for up to 30% of the total C&DW, the application of RCP as a replacement material in concrete production has been scarce. RCP is a powdery material with particles below 150  $\mu\text{m}$  and is obtained by mechanical pre-treatment of C&DW through crushing, grinding, and sieving. The physical properties and chemical composition of RCP are shown in Tables 15 and 16. As can be observed from Table 16, the silica content is different in each source of RCP. The RCP from the source in ref. [173] originated from the concrete waste of a beam used in a railway traffic project. In contrast, the RCP from the source in ref. [174] was acclaimed from demolishing a 40-year-old building, which was built with grade C25 and no pozzolanic materials, whereas the RCP used in the research in ref. [175] was obtained by crushing the concrete waste obtained from demolishing a 20-year-old building.

**Table 15.** Physical properties of RCP [173].

Property	OPC	RCP
Bulk Density ( $\text{kg}/\text{m}^3$ )	1056	856
Apparent Density ( $\text{kg}/\text{m}^3$ )	2978	2355
Specific Surface Area ( $\text{cm}^2/\text{g}$ )	4930	4670

**Table 16.** Comparison of chemical compositions of RCP and FRCA with OPC (Note: Sum \* is the sum of pozzolanic oxides).

Oxides (%)	SiO <sub>2</sub>	Al <sub>2</sub> O <sub>3</sub>	Fe <sub>2</sub> O <sub>3</sub>	Sum *	CaO	MgO	Na <sub>2</sub> O	K <sub>2</sub> O	SO <sub>3</sub>	LOI	Ref
OPC	19.57	3.81	3.12	26.5	64.51	1.48	-	0.69	5.43	1.08	[167]
FRCA	57.37	9.64	3.27	70.28	17.9	0.59	-	3.41	1.53	5.61	[167]
RCP	27.8	6.7	2.73	37.23	29.1	4.49	0.56	1.09	1.11	-	[173]
	55.19	2.18	4.85	62.22	35.02	0.29	0.22	0.7	0.51	1.42	[174]
	64.81	7.77	1.59	74.17	19.14	1.54	1.76	2.94	-	-	[175]

Rakhimova and Rakhimov [176] observed that RCP has a mixed mineral composition of quartz, calcite, ettringite, unhydrated OPC, calcium silicates, and aluminate hydrates. The presence of unhydrated OPC makes RCP a promising SCM [175]. Kim and Choi [177] utilized two types of RCP with different Blaine fineness values (928 and 1360  $\text{cm}^2/\text{g}$ ). The microstructural analysis revealed that the shape of RCP particles was angular and identical to that of cement particles; however, RCP particles were larger than cement particles and the surface of the particles contained hydrated products. As observed from Figure 4, the compressive strength decreases with the increase in RCP proportion, irrespective of fineness. With 15% RCP, the strength loss at 28 days compared to the reference was 25–28%, while it was 64–73% for 45% RCP. The significant loss in compressive strength was attributed to RCP consisting of non-reactive powders. Zhu et al. [178] studied the impact of 30% RCP (produced by crushing and grinding brick and concrete waste) on the concrete's properties. Concrete with RCP developed strength faster than concrete with FA at a younger age, which was attributed to the unhydrated cement particles in RCP. Sun et al. [179] evaluated the effect of RCP on mortar properties with and without spontaneous combustion gangue powder (SCGP). Mortars with 30% and 50% RCP had compressive strengths of 17.87 and 14.57 MPa, respectively, compared to 26.13 MPa for the control mix. Meanwhile samples with 15% and 25% RCP combined with SCGP had compressive strengths of 22.85 and 14.99 MPa, respectively, after 28 days. As shown in Figure 5, RCP-containing mixes contain inert particles, which reduce the total binder activity and hydration products, causing micro-cracks and strength loss. RCP's lower pozzolanic reactivity and fineness increase the chloride penetration, thus it can be observed that a higher pozzolanic activity material such as SCGP may be utilized along with RCP to achieve better strength.

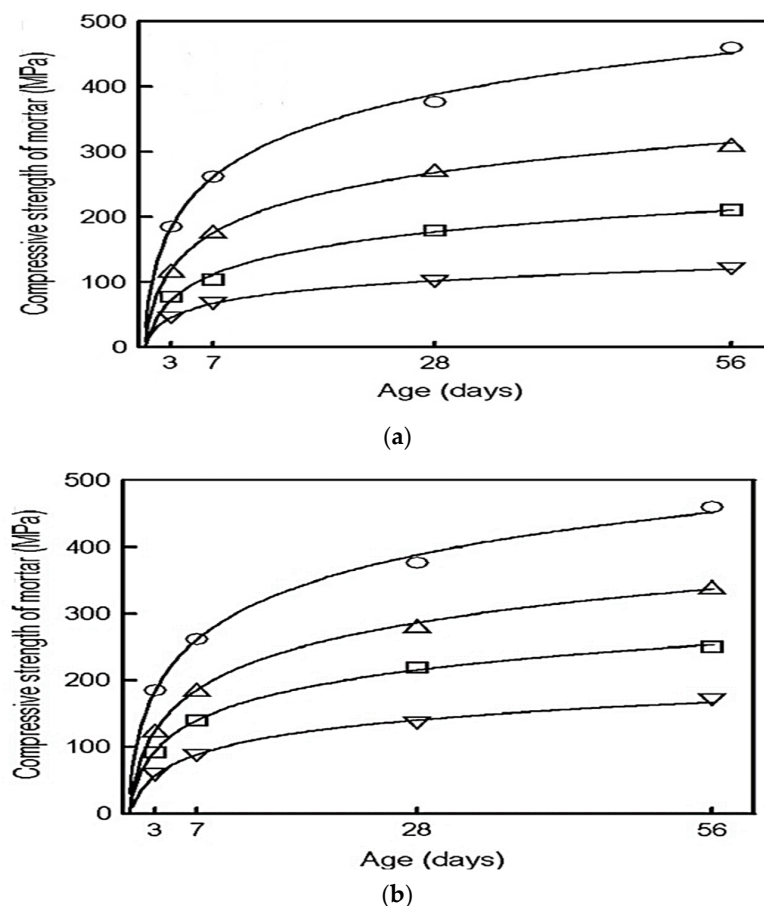


**Figure 4.** Influence of RCP on the compressive strength of mortar with RCP with (a) Blaine fineness of 928  $\text{cm}^2/\text{g}$  and (b) Blaine fineness of 1360  $\text{cm}^2/\text{g}$  (Note:  $\circ$  = reference mortar,  $\triangle$  = 15% RCP,  $\square$  = 30% RCP and  $\nabla$  = 45% RCP) [177].

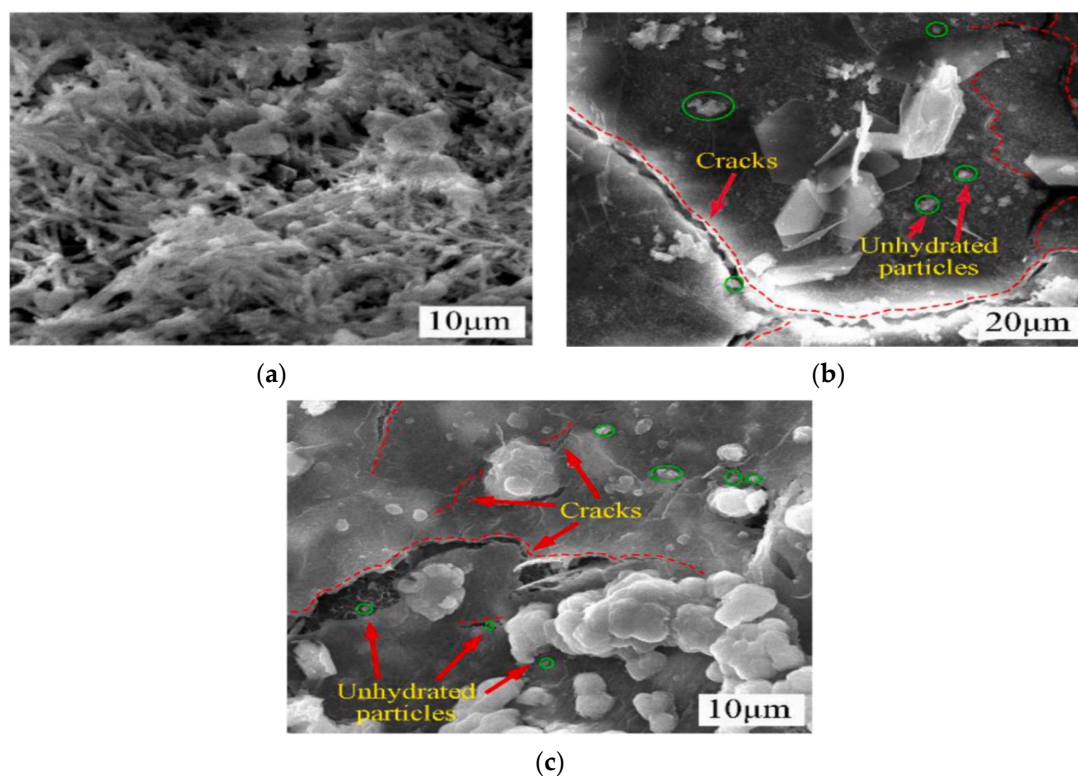


**Figure 5.** SEM images of mortar consisting of (a) OPC (b) 30% RCP and (c) 50% RCP [170].

Based on the present literature, it can be concluded that RCP has the potential to be used as an SCM as it provides additional nucleation sites which in turn accelerates the hydration of cement [180] and thus enhances the strength [181,182].

### 2.5. Insight on the Emerging SCMs

The purpose of utilizing SCMs in concrete is to reduce the overall project (materials) costs and environmental burdens. The existing SCMs have thus far achieved both objectives. Although various SCMs have been evaluated, their use in construction has not been optimized. The industry has been more comfortable with established SCMs, such as FA, GGBS, SF, and LP. With the imminent closure of coal plants, causing FA supply (700–1100 million tonnes per annum) restriction, the construction industry is looking for a global alternative.

Emerging SCMs are so diverse that determining their concrete performance is difficult. Emerging SCMs face challenges with current SCM test methods. Existing SCMs have dedicated standards and quality requirements, such as ASTM C618 [25] and EN 450-1 [26] for FA, standard ASTM C989-06 [183] and EN 15167-1 [184] for GGBS, standard IS 15388 [185], EN 13263-1 [186], and ASTM C1240-20 [187] for SF, and standard ASTM C1797-17 [188] for LP. Existing standards and methods are unsuitable for evaluating new SCMs since their chemical and mineralogical composition and poorly crystalline phase structure must be understood.

With 3.25 billion tonnes of metallic ore mined annually, mine tailing waste is considerable. According to their chemical composition, most mine tailings are pozzolanic. However, their low pozzolanic reactivity negatively affects concrete properties when used without pre-treatment. The EPA classifies AD as a highly flammable, non-corrosive hazardous material. Recycled AD contains toxic materials, thus landfilling them is not ecologically fair. However, this refers to their disposal in raw form; these hazards could be mitigated if they are utilized as SCMs.

Unbound applications such as road construction are the main use of BOF slags. They can partially replace concrete binders. Before reusing slag, free CaO and MgO must be removed to prevent volumetric instability. EAF slag can be used as a partial binder to create

concrete with similar or higher mechanical properties than conventional concrete. However, short- and long-term studies are still needed before industrial application. LF slag has not worked well as an SCM due to its volumetric instability, tendency to self-pulverize during cooling, and low hydraulic properties. According to some studies, using alkaline activators and cooling LF slags may help achieve comparable mechanical strength in concrete. More lab and industrial research are needed [133].

CSW in concrete requires a technological breakthrough, as the utilization as SCM has been limited and results indicate that preconditioning is required before mixing to achieve better results. It is not a ready-to-use material that can be taken from landfills and immediately used in concrete. This may limit the use of CSW as an SCM. Variations in physical and chemical properties cause RCP concrete to have different mechanical and durability properties. RCP as an SCM requires quality control to achieve the desired results, but a lack of well-developed guidelines hinders its industrial adoption [189].

Regarding the quantity of emerging SCMs, the volume of CSW generation can vary between 165–330 million tonnes depending on the total global concrete production. In comparison, 4 million tonnes of primary AD and 1 million tonnes of secondary AD are produced annually. It is estimated that 160–240 million tonnes of BOF slags and 104 million tonnes of EAF slag are generated annually. The mining sector produces 5–7 billion tonnes of mine tailings annually. Despite the emerging SCMs having more than enough yield volume to replace the existing SCMs, which are waste materials, the main hindrance to their utilization is their supply to cement factories and concrete producers. This is because China accounts for more than half of all steel and aluminum production in the world and is also a leading producer in other metal production. The waste materials are primarily available free of charge; however, the supply of waste materials such as mine tailings, ADs, and slags to cement factories and concrete producers has associated costs and embodied carbon within it. The distance between the source of SCMs and the cement factories and concrete producers is closely related to transportation costs and embodied carbon, and can thus impact the objective.

Each emerging SCM has different physical properties and chemical composition while some have low reactivity; therefore, their use will be limited to small-scale applications and pilot projects. Literature on emerging SCMs suggests they could be the next FA or GGBS; however, more extensive testing is needed under different durability and environmental protection conditions and life cycle assessments are required to evaluate the environmental impact of emerging SCMs depending on the region.

### 3. Methods for Enhancing the Reactivity of SCMs

Most materials utilized as potential SCMs are waste materials; therefore, they are of sub-optimal quality [190]. If untreated, these waste materials can negatively affect the properties of concrete (especially its strength). Past research has described solutions to this problem by employing various pre-treatment techniques and methods to enhance the reactivity of SCMs.

#### 3.1. Reduction in Particle Size of SCMs

Tangchirapat et al. [191] asserted that the quality of the binding material used in concrete production influences its strength. To increase the pozzolanic activity, the material must be ground into fine particles. The ground particles have higher surface areas, thus creating additional nucleation sites during hydration, which results in the development of C-S-H layer formation. Initially, nano-silica was used, and research has continued to date [192–194] but is being expanded to include other nano-sized particles, such as natural pozzolans [195], clays, and other potential materials used as SCMs or nucleation enhancers [196]. An ultrafine powder can be made using standard laboratory equipment such as ball mills and vibratory disc mills. Grinding reduces the particle size and increases the specific surface area, affecting the internal structure and physical and chemical properties.

As mentioned earlier, mine tailings have low reactivity but the reactivity of different components, such as Al, Si, Fe, Mg, and Ca, can be improved and the particle shape and homogeneity can be changed by mechanically grinding mine tailings [197]. The grinding of phyllite mine tailings for three hours caused Al and Si to become 93% and 23% soluble, while the XRD analysis revealed a less intense albite peak but no new phases [198]. A vertical planetary ball mill was used to grind iron ore tailings in another study [199], which caused the specific surface area to increase from 103 m<sup>2</sup>/kg (raw iron ore tailings) to 463 m<sup>2</sup>/kg (20-min grinding) and 581 m<sup>2</sup>/kg (ground for 40 min).

CSW contains calcium-silicate, which is a potential cementitious material, and the exposure of CSW to CO<sub>2</sub> and water during storage causes the calcium phases to react and form calcium carbonate and incompact C-S-H, which reduces its potential reactivity. As observed in Figure 6, it was found that wet milling has the potential to increase the reactivity of CSW. CSW, water, and zirconia balls were placed in a vertical stirring mill and milled for 20, 40, and 60 min [169]. The wet-milled CSW curves became narrower than those of unground CSW over time. Wet milling achieved minimum and maximum particle of 300 nm and 10 μm, respectively. No sand or gravel remained after wet milling, indicating that all large particles were ground fine, while the pH dropped from 11.53 to 10.55 in 60 min. There was an increase in the carbonation reaction of C-S-H during wet milling, resulting in a decline in alkalinity [169]. A similar fineness to cement is required if WWA [152] is to be used as a cementitious material. Therefore, WWA also needs to be ground [152]. However, the grinding time may vary depending on the type of WWA and ash quality.

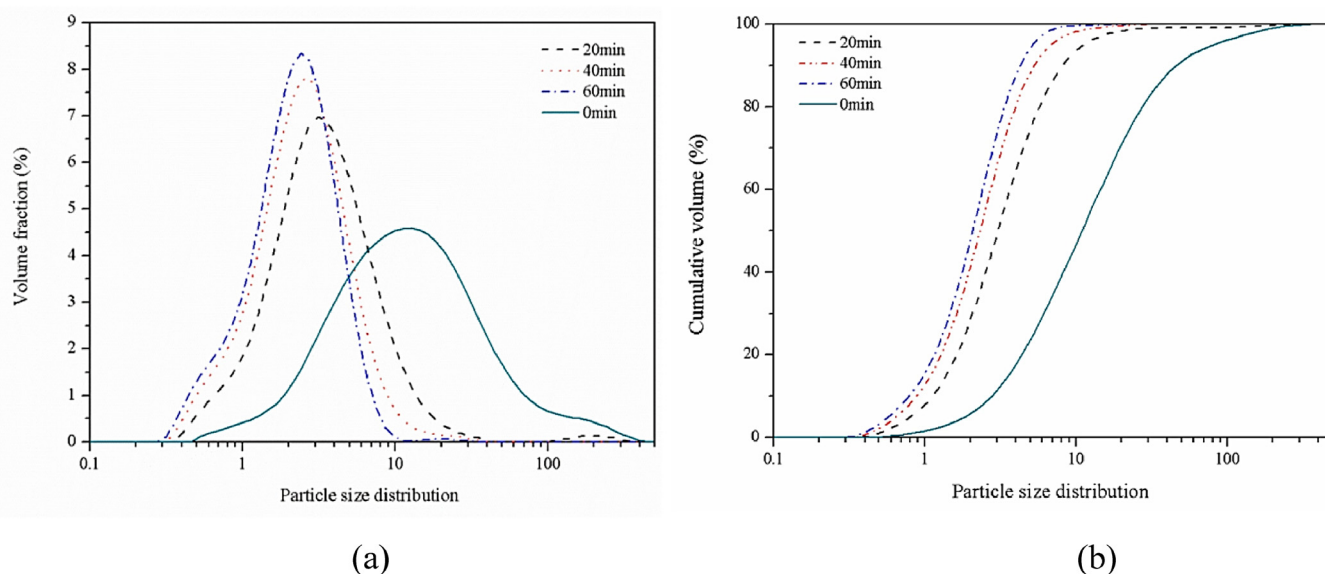


**Figure 6.** The particle size distribution (μm) of CSW (a) volume fraction (%) and (b) cumulative volume (%) with respect to grinding duration [169].

While finer SCMs, especially those with nanoparticles, have higher reactivity, they are difficult to disperse in concrete and therefore do not always work well as cementitious materials in concrete. Various researchers have tried to solve the lack of particle dispersion. Rodriguez et al. [200] used high-frequency ultrasonication to disperse SF particles in water. Consumption of portlandite increased, as did the formation of C-S-H with a longer chain length and lower Ca:Si ratio than with densified SF. Kawashima et al. [201] used sonication and chemical admixtures to improve the dispersion of nano-calcium carbonate.

### 3.2. Thermal Treatment

Thermal treatment can also improve the reactivity of potential SCMs. The optimization of the calcination process has recently gained attention, particularly in optimizing temperature and time for calcination. The reactive amorphous silica phase can be activated

or achieved by calcining or incinerating various clays, which influences the particle size distribution (PSD) [202]. However, incinerating beyond a certain temperature may convert the amorphous silica into crystalline silica [203], consisting of cristobalite and tridymite, which reduces the pozzolanic reactivity. Calcination and aeration increase the reactivity of mine tailings [204,205]. During calcination, the crystalline structure is ruptured, minerals are decomposed, and amorphous phases with high pozzolanic activity are formed [206,207]. Perumal et al. [205] studied the thermal treatment of phosphate, kaolinite, and lithium tailings. According to XRD, phosphate mine tailings contain phlogopite, calcite, tremolite, and dolomite. The calcite decomposed to form CaO at 750 °C. First-stage calcination boosted reactivity by forming CaO and reducing crystallinity. Quartz and silicates formed during the second calcination stage, reducing reactivity. Perumal et al. [205] found that kaolinite decomposed at 750 °C, forming metakaolin. Metakaolin's amorphous structure was undetectable by XRD [205]. At 900 °C, the albite peak's intensity decreased, indicating partial decomposition in lithium tailings. The phase changes suggested that phosphate mine tailings are more reactive after calcination than kaolinite and lithium tailings.

### 3.3. Additives

Inorganic additives have been found to increase the pozzolanic reactivity of SCMs. Ghorbel and Samet [208] added iron content (10, 25, 50, and 150 mL of 0.4 M  $\text{Fe}(\text{NO}_3)_3 \cdot 9\text{H}_2\text{O}$  solution) to kaolinitic sheets. The XRD analysis exhibited the formation of hematite ( $\text{Fe}_2\text{O}_3$ ) and goethite ( $\text{FeO}(\text{OH})$ ) in the metakaolin, while the compressive strength revealed that up to 2.7%  $\text{Fe}_2\text{O}_3$  increased the pozzolanic activity of the metakaolin. Soro [209] also studied the influence of iron additives on kaolin's thermal changes and found that when iron was added to kaolin, it precipitated as ferrihydrite and did not participate in the dihydroxylation (addition of hydrogen to a hydroxyl (alcohol) group creating water and an alkyl group) of kaolinite. Nevertheless, iron ions diffused into metakaolin at temperatures higher than 900 °C during the heating process. The ferrihydrite particles that formed at 300 °C became hematite. Taylor-Lange et al. [210] added zinc oxides to clays such as kaolinite, montmorillonite, and illite before and after calcination, reporting similar results. Using metakaolin with addition of zinc oxide increased the 28-day compressive strength but not when calcined montmorillonite and illite were used instead. It was found that the combination of zinc oxide and calcined clays reduced the cement hydration retardation that is typically observed with zinc oxide additions, which was unexpected, since the zinc oxide behaved quite like sucrose, acting as a retarder in the absence of metakaolin.

### 3.4. Combined Treatments

Recent research has shown that chemical treatment before combustion improves the properties of SCMs. Vaughan et al. [211] used hydrochloric acid to leach metals and alkalis from rice husks before calcination. A total of 6 kg of rice husks were boiled in 60 L of 0.01 N hydrochloric acid (HCl) solution for an hour. The material was then washed with tap water to neutralize the pH and dried for three days at room temperature. This was performed to determine the effects of acidic pre-treatment on the SCM. The acid-treated and non-acid-treated rice husks were then control-burned at constant temperature. The ground ash was added to saturated  $\text{Ca}(\text{OH})_2$  solutions and the solutions' time-dependent electrical conductivity was measured; pH determined the ash's pozzolanic reactivity. Additionally, the compressive strength activity was calculated. Acid-treated ash had higher  $\text{SiO}_2$  content, lower alkalinity and unburned carbon content, better grindability, and smaller particle size than non-acid-treated rice husks. This made the lime more reactive and less sensitive to prolonged combustion times. Vaughan et al. [211] concluded that rice husk treatment using 0.01 N HCl was sufficient. Ata and Riding [212] used hydrothermal and thermochemical pre-treatments on rice and wheat straw ashes for utilization in concrete. Samples were exposed to hydrothermal pre-treatment using distilled water, thermochemical pre-treatment with 0.1 N HCl, and further thermal treatment in an electric muffle furnace at various temperatures and times. Finally, a ball mill was used for an hour at 85

rpm. The pre-treatments reduced the Ca, K, and Mg contents and increased the amorphous silica content and surface area. Moreover, higher temperatures increased the effectiveness of Ca, K, and Mg, thereby improving the pozzolanic activity.

To our knowledge, combined treatment has not been employed for emerging SCMs; however, the above mentioned effectiveness of the combined treatment on existing SCMs indicates that a similar effect could be achieved when employed to treat the emerging SCMs discussed in this article.

#### 4. Reactivity Assessment Methods

SCMs are by-products or waste of other industrial processes, and, as such, their quality has traditionally been subservient to the overall industrial productivity. This has led to the production of low-quality SCMs and considerable variability between sources, which has made it challenging to keep source quality consistent over time [190]. Therefore, the first step in evaluating emerging materials as potential SCMs is determining their characteristics. Various methods are used to determine SCM characteristics, such as: (1) a laser diffraction analyzer is used to determine the PSD, indicating the range of particle sizes. (2) X-ray fluorescence spectroscopy is used to determine the chemical/oxide composition of potential SCMs in order to define whether they are latent hydraulic or pozzolanic. Pozzolanic SCMs are classified according to ASTM C618 [25] or Rankin classification based on the  $\text{CaO}/\text{SiO}_2$  ratio with:  $<0.5$  is pozzolanic,  $1\text{--}1.5$  is latent hydraulic, and  $>2$  is hydraulic [213]. (3) X-ray diffraction analysis is used for qualitative and quantitative analysis of mineral composition.

To evaluate the reactivity of SCMs, a wide range of standardized and non-standardized methods have been utilized. In general, these methods can be divided into two categories, i.e., direct methods measuring physical properties or indirect methods measuring chemical properties. The widely used reactivity evaluation methods of SCMs as shown in Table 17.

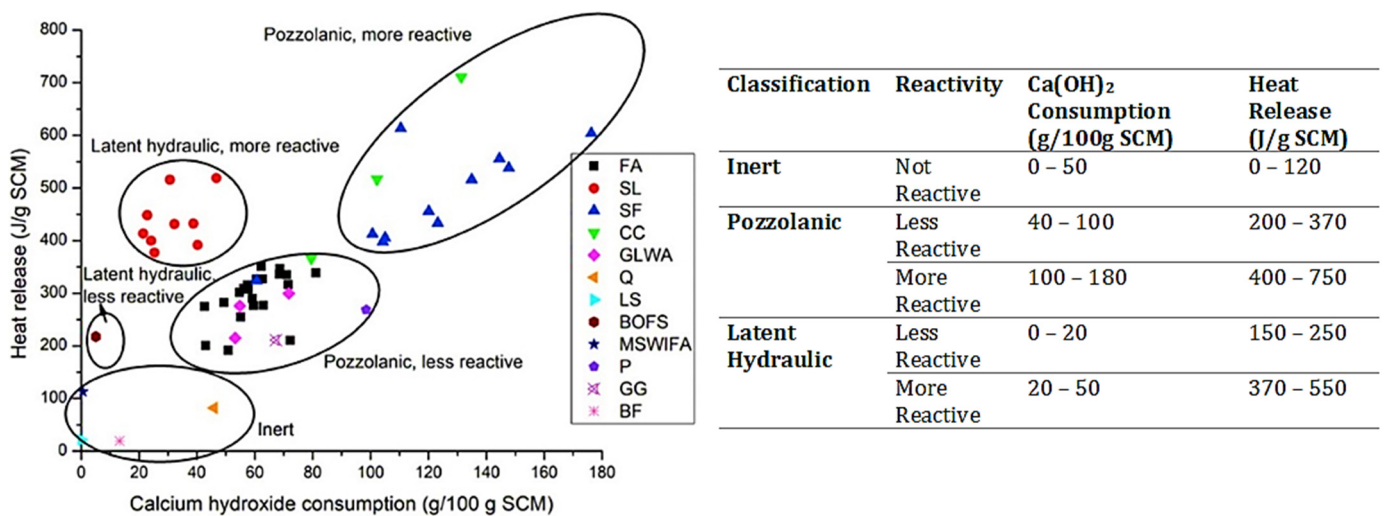


**Figure 7.** Classification of SCMs by plotting the heat release against  $\text{Ca}(\text{OH})_2$  consumption [229] (FA = Class C and Class F fly ash; SL = ground granulated blast furnace slags; SF = silica fume; CC = calcined clay; GLWA = ground lightweight aggregate; Q = quartz; LS = ground limestone; BOFS = basic oxygen furnace slag; MSWIFA = municipal solid waste incineration fly ash; P = ground pumice; GG = ground glass; BF = basalt fines).

Table 17. Different reactivity test methods for SCMs.

Test	Ref	Procedure	Remarks
Frattini Test EN 196-1 Part 5	[214]	<ul style="list-style-type: none"> <li>- Samples are prepared or mixed, stored for 7 and 28 days at a temperature of 40 °C, after which the samples are allowed to cool down to room temperature (27 °C), and the solution is filtered in a vacuum before testing.</li> <li>- The filtrate is then titrated with 0.1 M hydrochloride acid, EDTA, and murexide indicators are applied to detect OH<sup>-</sup> and Ca<sup>+</sup> ion concentrations.</li> </ul>	<ul style="list-style-type: none"> <li>- If an SCM is reactive, the calcium ion concentration will be below saturation at the specified OH<sup>-</sup> ion concentration.</li> </ul>
Chapelle Test and Modified Chapelle Test (NF P18-513)	[215]	<ul style="list-style-type: none"> <li>- 1 g of the SCM is mixed with 1 g of Ca(OH)<sub>2</sub> in 200 mL water heated at 90–100 °C for 16 h, after which the unreacted lime is examined, and the results are expressed in milligrams of Ca(OH)<sub>2</sub> per unit of SCM, respectively. The Ca(OH)<sub>2</sub> consumed in mg/g of SCM is calculated using Equation (1):  <math display="block">SCM_{reactivity} = \frac{a-b+c}{d} \times 74000 \quad (1)</math> </li> <li>- In the modified Chapelle test, 1 g of SCM is mixed with 2 g of Ca(OH)<sub>2</sub>.</li> <li>- This method produces two blank solutions using the same setup: (1) distilled water and Ca(OH)<sub>2</sub> and (2) distilled water and SCM [216].</li> <li>- The first blank solution is used to correct for carbonation while the second blank solution corrects for the release of alkali from the SCM.</li> </ul>	<ul style="list-style-type: none"> <li>- The variability of the Chapelle test and modified Chapelle test is reduced due to the use of CH instead of OPC.</li> <li>- An increase in the reactivity and modification of kinetics of the specimens has been observed to be due to the SCMs being subjected to high temperature (90–100 °C) for a significant duration (16 h).</li> <li>- Neither test takes into consideration the calcium already present in slag specimens.</li> </ul>
R3 Calorimetry	[217]	<ul style="list-style-type: none"> <li>- The powder and water are pre-conditioned separately overnight at 40 °C in the calorimeter, after which they are mixed in a mechanical mixer for 2 min. Afterwards, a glass ampoule is weighed together with 15 g of sample, which is then sealed and inserted in the calorimeter at a constant temperature of 40 °C for 7 days to record the heat.</li> </ul>	<ul style="list-style-type: none"> <li>- The SCM is mixed with Ca(OH)<sub>2</sub>, sulphates, and alkalis in the quantities [218] initially used to evaluate calcined clays and limestone mixes, but its popularity has grown such that it is used for all SCMs.</li> <li>- The measured heat of hydration correlates well with mortar strength development, tested on calcined clay and limestone mixes [215].</li> </ul>
R <sup>3</sup> Bound Water	[217]	<ul style="list-style-type: none"> <li>- Sliced specimens extracted from 7 days hydrated samples are dried at 105 °C to remove any surface and pore water, afterwards furnace-heated at 400 °C for 2 h, the weight loss is measured and recorded.</li> </ul>	<ul style="list-style-type: none"> <li>- The weight loss is proportional to the amount of water present in hydration products such as C-S-H and C-A-S-H, and this water helps define how the SCM reacts.</li> <li>- Additional step was added in ASTM C1897 [219]: once the weight loss is recorded at 400 °C, the sample is put in an oven at 500 °C and weight loss is recorded again.</li> <li>- By prolonging the temperature between 400 and 500 °C, CH content may be estimated.</li> </ul>
R <sup>3</sup> Chemical Shrinkage	[217, 220]	<ul style="list-style-type: none"> <li>- Freshly prepared paste samples are poured into a vial up to 3 cm, afterwards the vial is completely filled with 40 °C temperature de-aerated water.</li> <li>- The sealed samples are then placed in water bath of constant temperature of 40 °C. The change in volume is noted, and based on the volumetric change, the chemical shrinkage is calculated.</li> </ul>	<ul style="list-style-type: none"> <li>- This R<sup>3</sup> model test has the advantage of being repeatable for more extended periods than most other R<sup>3</sup> test methods and has been employed in evaluating blends of SCMs with lime in a 1:1 ratio at a constant room temperature of 27 °C.</li> <li>- The volumetric change can be recorded in small intervals during the early stage, and the testing duration can last for up to 14 days.</li> </ul>

Table 17. Cont.

Test	Ref	Procedure	Remarks
R <sup>3</sup> Portlandite Consumption	[217]	- Pastes are prepared and dried at 40 °C for 7 days and weighed. - 50 mg of powder is heated from 30 to 950 °C at 10 °C/min in a TGA, and the weight loss over temperature is recorded.	- Portlandite consumption is computed using the tangent approach given by Scrivener et al. [221], and portlandite consumption is calculated by difference to the initial content [217].
Suraneni (Modified R <sup>3</sup> Isothermal Calorimetry) Test	[222]	- Paste samples, prepared by mixing Ca(OH) <sub>2</sub> and SCM in a 3:1 mass ratio with 0.5 M KOH to maintain 0.9 liquid-solid ratio of 0.9, are placed in a 50 °C preconditioned calorimeter, and the heat release is recorded for 240 h. - 50 mg of SCM is heated from 23 to 500 °C at 10 °C/min in a TGA	- Classified SCMs based on Ca(OH) <sub>2</sub> consumption and heat release (Figure 7). - The boundaries suggested in Figure 7 for heat release are not fundamental, as a slight change in the system model (Ca(OH) <sub>2</sub> value and temperature) can cause different values.
Lime Reactivity IS 1727-1967	[223]	- Mortar samples consisting of SCM, Ca(OH) <sub>2</sub> and sand at a ratio of 1:2M:9, where M is the SCM/CH specific gravity ratio are prepared and kept at 27 °C for 48 h. After 8 days at 50 °C temperature and 90% relative humidity, the specimens' compressive strengths are evaluated and dubbed the SCM's lime reactivity.	- The fluctuating water to powder ratio and SCM concentration makes it impossible to compare similar SCMs with varying physical properties, let alone different SCMs. Thus, modified lime reactivity test in which lime to SCM ratio is set at one based on the lime reactivity test quantities 0.67 w/b ratio to eliminate mix fluctuation.
Heat of Hydration (1:1) Test	[224]	- The paste specimen (SCM and lime at 1:1 with 0.65 w/b ratio) is placed in an isothermal calorimeter at 27 °C for 7 days, during which time its heat of hydration is measured.	- In contrast to R <sup>3</sup> calorimetry, heat of hydration does not restrict the system to pozzolanic reactions and by conducting the tests at an ambient temperature, the effects of a higher temperature and kinetics can be reduced, leading to more reliable results.
Strength Activity Index (SAI) ASTM C311	[225]	- The compressive strength of concrete/mortar containing SCM is compared with the compressive strength of reference concrete/mortar sample at different curing ages. The influence of SCM can be expressed in Equation (2). $SAI = \frac{CS_{SCM}}{CS_{ref}} \quad (2)$	- To comply with ASTM C618 [25] and EN 450-1 [26], SAI of at least 75% of the control mixture after 7 or 28 days is required. - It fails to distinguish between reactive and inert materials due to higher SCM level; the filler effects may outweigh other reaction effects [226], thus testing at early age may be impractical since pozzolanic activity is low at early age, often indistinguishable from inert fillers [227]. Additionally, the 75% cap is too low, as when cement is diluted, the strength of the test sample can be 80% of the control at the same w/c ratio [228].

Note: SCM reactivity = activity of SCM in mg of Ca(OH)<sub>2</sub> per g of SCM; a = moles of Ca(OH)<sub>2</sub> for reaction products and carbonation; b = moles of Ca(OH)<sub>2</sub> for carbonation; c = moles of Ca(OH)<sub>2</sub> from SCM itself; d = weight of SCM; KOH = potassium hydroxide; SAI = strength activity index; CS<sub>SCM</sub> = compressive strength of specimen incorporating SCM; CS<sub>ref</sub> = compressive strength of referent specimen.

#### Insight on the Evaluation Methods

SCMs are primarily inorganic materials that, when combined with Portland cement, contribute to the properties of the hardened concrete through a chemical reaction, such as hydraulic or pozzolanic activity. The application of existing SCMs, such as FA, slags, and other such materials, is growing at an exponential rate. However, the supply of such SCMs is becoming restricted, thus newer materials are emerging as potential SCMs. The utilization of SCMs has been linked to an improvement in the workability, mechanical, and durability performance of concrete. On the other hand, it is common knowledge that the reactivity of SCMs plays a significant role in ensuring that there is an improvement in the performance of the concrete. Because there is a growing demand for cementitious products that are more environmentally friendly, it is becoming increasingly important to

evaluate the pozzolanic activity of cement replacement materials. The reactivity of SCMs has been determined using conventional reactivity methods, such as Chapelle's test and the modified Chapelle's test. However, these experiments have certain drawbacks that are caused by the very accelerated settings, as well as the high degree of divergence from actual conditions (i.e., high water content and the solution solely comprises  $\text{Ca}(\text{OH})_2$ ).

To avoid such problems, newer methods, known as  $R^3$ , have been introduced. Recently, comparative analysis [217] has been conducted on some of the different reactivity methods mentioned in Table 17. Different SCMs were evaluated, and it was observed that the decades-old, standardized methods exhibited weak correlations for relative compressive strength. A correlation  $R^2 \geq 0.85$  is acceptable, which was only found for  $R^3$  calorimetry and  $R^3$  bound water, as shown in Figure 8. It was also observed that when slag SCMs were omitted, the correlations for the Frattini and modified Chapelle tests increased such that the  $R^2$  values became more acceptable. Furthermore, the lime reactivity test gave a reasonable correlation for strength gains after 90 days due to pozzolanic activity. The  $R^3$  model tests had the highest reproducibility of the methods studied, and their reproducibility could likely be increased by providing more specific details about the execution of the tests.

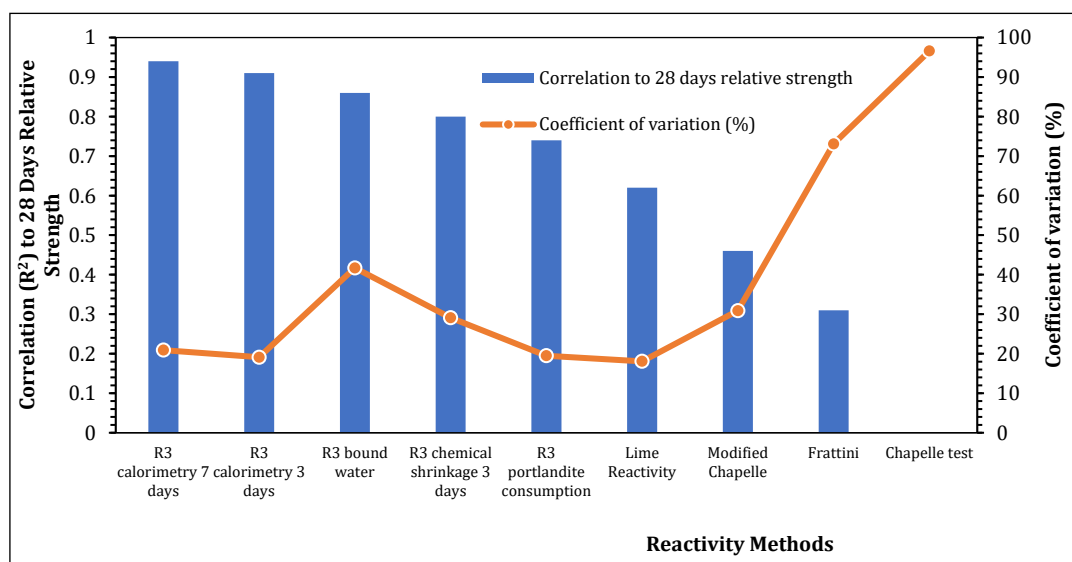


Figure 8. Summary of different reactivity methods [217].

Although these reactivity evaluation methods have been used on existing SCMs, they may also be employed to evaluate the reactivity of new SCMs. Compared to existing SCMs, some of the newer SCMs may lack reactivity, resources, and have increased requirements for quality control. These factors make it more difficult for new SCMs to be adopted, even though their technical potential is enormous. Therefore, it is imperative that new SCMs be evaluated before being incorporated into either existing or newly developed standards to facilitate their widespread application in the years to come.

## 5. Conclusions

The objective of this study was to present emerging and new SCMs as an alternative to the existing SCMs, the supply of which is expected to be reduced soon due to the closure of coal plants and recycling initiatives in the steel and iron industries. In this regard, waste materials from concrete and timber production are increasing in quantity and can be utilized as SCMs. Furthermore, wastes such as mine tailings and steel slags have had limited application, although they have presented themselves as emerging SCMs. Based on the review, the following conclusions are drawn:

1. When unprocessed, certain materials such as CSW and AD are considered as hazardous; however, when used as an SCM in limited content, their hazardous nature is restricted and they can be beneficial for the construction industry.
2. The only environmental impact and cost associated with emerging SCMs is the transportation of SCMs from the source to cement industries.
3. The huge volume of emerging SCMs could potentially surpass the utilization of existing SCMs in concrete.
4. Pre-treatment to mechanically reduce particle size, calcining, and adding gypsum and iron increase reactivity. For decades, mechanically reducing SCM particle size has been the most effective treatment method for improving reactivity, but it increases specific surface area and water demand. The CO<sub>2</sub> emissions from these treatment methods may be acceptable when the reactivity of SCMs is enhanced.
5. Several methods can be used to determine the material's reactivity. As a rapid screening method, physical properties and chemical composition are used to classify a material as a potential SCM. However, some materials, such as mine tailings, may have pozzolanic oxides that have low pozzolanic reactivity because they are crystalline. This lowers the mechanical and durability properties of the concrete. Therefore, the reactivity of SCMs must be studied.
6. Existing SCM reactivity methods have significant limitations. Due to these limitations, the actual reactivity of emerging SCMs is unknown or underreported, which prevents emerging SCMs from reaching the market.

The lack of studies on the short-term and long-term effects of incorporating emerging SCMs in concrete has also been one of the reasons for SCMs not being used on an industrial scale. Therefore, further research on the mechanical and durability properties is needed to propose the implementation of such emerging SCMs for industrial applications. Based on those results, a comprehensive standard may be prepared. Additionally, the supply of emerging SCMs to cement factories may adversely influence their sustainability, thus regional economic and environmental assessments throughout the materials' life cycles should be conducted.

**Author Contributions:** Conceptualization, A.A.J. and I.N.; methodology, A.A.J., I.N. and E.G.; formal analysis, A.A.J.; investigation, A.A.J.; data curation, A.A.J.; writing—original draft preparation, A.A.J., I.N. and E.G.; writing—review and editing, A.A.J., I.N. and E.G.; supervision, I.N. and E.G.; project administration, I.N.; funding acquisition, I.N. All authors have read and agreed to the published version of the manuscript.

**Funding:** The outcome has been achieved with the financial support of the Circulus Project Nr. 299322 funded by the Norwegian Research Council.

**Conflicts of Interest:** The authors declare no conflict of interest.

## References

1. Rashad, A.M.; Bai, Y.; Basheer, P.A.M.; Milestone, N.B.; Collier, N.C. Hydration and properties of sodium sulfate activated slag. *Cem. Concr. Compos.* **2013**, *37*, 20–29. [CrossRef]
2. CEMBUREAU. Cementing the European Green Deal, Reaching Climate Neutrality along the Cement and Concrete Value Chain by 2050. 2020. Available online: [https://cembureau.eu/media/kuxd32gi/cembureau-2050-roadmap\\_final-version\\_web.pdf](https://cembureau.eu/media/kuxd32gi/cembureau-2050-roadmap_final-version_web.pdf) (accessed on 25 May 2022).
3. Xi, F.; Davis, S.; Ciaia, P.; Crawford-Brown, D.; Guan, D.; Pade, C.; Shi, F.X.T.; Syddall, D.C.-B.M.; Lv, J.; Ji, L.; et al. Substantial global carbon uptake by cement carbonation. *Nat. Geosci.* **2016**, *9*, 880–883. [CrossRef]
4. International Energy Agency. *Global Energy & CO<sub>2</sub> Status Report 2019—Analysis*; International Energy Agency: Paris, France, 2019; Available online: <https://www.iea.org/reports/global-energy-co2-status-report-2019> (accessed on 4 February 2021).
5. UN Environment; Scrivener, K.L.; John, V.M.; Gartner, E.M. Eco-efficient cements: Potential economically viable solutions for a low-CO<sub>2</sub> cement-based materials industry. *Cem. Concr. Res.* **2018**, *114*, 2–26.
6. Yang, K.-H.; Jung, Y.-B.; Cho, M.-S.; Tae, S.-H. Effect of supplementary cementitious materials on reduction of CO<sub>2</sub> emissions from concrete. *J. Clean. Prod.* **2015**, *103*, 774–783. [CrossRef]
7. Mala, K.; Mullick, A.K.; Jain, K.K.; Singh, P.K. Effect of Relative Levels of Mineral Admixtures on Strength of Concrete with Ternary Cement Blend. *Int. J. Concr. Struct. Mater.* **2013**, *7*, 239–249. [CrossRef]

8. Zhang, Q.; Ye, G. Dehydration kinetics of Portland cement paste at high temperature. *J. Therm. Anal. Calorim.* **2012**, *110*, 153–158. [CrossRef]
9. Gunnarsson, I.; Arnórsson, S. Amorphous silica solubility and the thermodynamic properties of  $\text{H}_4\text{SiO}_4$  in the range of 0° to 350 °C at Psat. *Geochim. Cosmochim. Acta* **2000**, *64*, 2295–2307. [CrossRef]
10. Izadifar, M.; Ukrainczyk, N.; Uddin, K.M.S.; Middendorf, B.; Koenders, E. Dissolution of Portlandite in Pure Water: Part 2 Atomistic Kinetic Monte Carlo (KMC) Approach. *Materials* **2022**, *15*, 1442. [CrossRef]
11. Izadifar, M.; Natzeck, C.; Emmerich, K.; Weidler, P.G.; Gohari, S.; Burvill, C.; Thissen, P. Unexpected Chemical Activity of a Mineral Surface: The Role of Crystal Water in Tobermorite. *J. Phys. Chem. C* **2022**, *126*, 12405–12412. [CrossRef]
12. Aprianti, E. A huge number of artificial waste material can be supplementary cementitious material (SCM) for concrete production—A review part II. *J. Clean. Prod.* **2017**, *142*, 4178–4194. [CrossRef]
13. Bediako, M.; Frimpong, A.O. Alternative Binders for Increased Sustainable Construction in Ghana—A Guide for Building Professionals. *Mater. Sci. Appl.* **2013**, *4*, 20–28. [CrossRef]
14. Habert, G.; Miller, S.A.; John, V.M.; Provis, J.L.; Favier, A.; Horvath, A.; Scrivener, K.L. Environmental impacts and decarbonization strategies in the cement and concrete industries. *Nat. Rev. Earth Environ.* **2020**, *1*, 559–573. [CrossRef]
15. Flower, D.J.M.; Sanjayan, J.G. Green house gas emissions due to concrete manufacture. *Int. J. Life Cycle Assess.* **2007**, *12*, 282–288. [CrossRef]
16. Juenger, M.C.G.; Snellings, R.; Bernal, S.A. Supplementary cementitious materials: New sources, characterization, and performance insights. *Cem. Concr. Res.* **2019**, *122*, 257–273. [CrossRef]
17. Zeggar, M.L.; Azline, N.; Safiee, N.A. Fly ash as supplementary material in concrete: A review. *IOP Conf. Ser. Earth Environ. Sci.* **2019**, *357*, 012025. [CrossRef]
18. Concreteproducts.com. Fly Ash Use in Concrete Up Slightly; Overall Ash Recycling Rate Down. 2020. Available online: <https://concreteproducts.com/index.php/2020/12/18/fly-ash-use-in-concrete-up-slightly-overall-ash-recycling-rate-down/> (accessed on 1 August 2022).
19. Amran, M.; Fediuk, R.; Murali, G.; Avudaiappan, S.; Ozbakkaloglu, T.; Vatin, N.; Karelina, M.; Klyuev, S.; Gholampour, A. Fly Ash-Based Eco-Efficient Concretes: A Comprehensive Review of the Short-Term Properties. *Materials* **2021**, *14*, 4264. [CrossRef]
20. Tapeshwar, K.; Ravi, R. A Review on Fly Ash Concrete. *Int. J. Latest Res. Eng. Comput.* **2015**, *3*, 7–10.
21. Flores, R.M. Coal Composition and Reservoir Characterization. In *Coal and Coalbed Gas*; Elsevier: Amsterdam, The Netherlands, 2014; pp. 235–299.
22. Blissett, R.S.; Rowson, N.A. A review of the multi-component utilisation of coal fly ash. *Fuel* **2012**, *97*, 1–23. [CrossRef]
23. Ahmaruzzaman, M. A review on the utilization of fly ash. *Prog. Energy Combust. Sci.* **2010**, *36*, 327–363. [CrossRef]
24. Amin, N.U. A multi-directional utilization of different ashes. *RSC Adv.* **2014**, *4*, 62769–62788. [CrossRef]
25. ASTM C618-19; Standard Specification for Coal Fly Ash and Raw or Calcined Natural Pozzolan for Use in Concrete. ASTM International: West Conshohocken, PA, USA, 2019.
26. EN 450-1; Fly Ash for Concrete—Definition, Specifications and Conformity Criteria. iTeh, Inc.: Newark, DE, USA, 2012.
27. Panesar, D.K. Supplementary cementing materials. In *Developments in the Formulation and Reinforcement of Concrete*; Elsevier: Amsterdam, The Netherlands, 2019; pp. 55–85.
28. Johari, M.M.; Brooks, J.; Kabir, S.; Rivard, P. Influence of supplementary cementitious materials on engineering properties of high strength concrete. *Constr. Build. Mater.* **2011**, *25*, 2639–2648. [CrossRef]
29. Behl, V.; Singh, V.; Dahiya, V.; Kumar, A. Characterization of physico-chemical and functional properties of fly ash concrete mix. *Mater. Today Proc.* **2021**, *50*, 941–945. [CrossRef]
30. Nath, P.; Sarker, P. Effect of Fly Ash on the Durability Properties of High Strength Concrete. *Procedia Eng.* **2011**, *14*, 1149–1156. [CrossRef]
31. Saha, A.K. Effect of class F fly ash on the durability properties of concrete. *Sustain. Environ. Res.* **2018**, *28*, 25–31. [CrossRef]
32. Islam, M.M.; Alam, M.T.; Islam, M.S. Effect of fly ash on freeze–thaw durability of concrete in marine environment. *Aust. J. Struct. Eng.* **2018**, *19*, 146–161. [CrossRef]
33. Zhang, J.; Matsuura, H.; Tsukihashi, F. Processes for Recycling. In *Treatise on Process Metallurgy*; Elsevier: Amsterdam, The Netherlands, 2014; pp. 1507–1561.
34. Matthes, W.; Vollpracht, A.; Villagrán, Y.; Kamali-Bernard, S.; Hooton, D.; Gruyaert, E.; Soutsos, M.; De Belie, N. Ground Granulated Blast-Furnace Slag. In *Properties of Fresh and Hardened Concrete Containing Supplementary Cementitious Materials State-of-the-Art Report of the RILEM Technical Committee 238-SCM, Working Group 4*; De Belie, N., Marios, S., Elke, G., Eds.; Springer: Cham, Switzerland, 2018; pp. 1–53.
35. World Steel Association. World Steel in Figures 2021. 2021. Available online: <https://worldsteel.org/wp-content/uploads/2021-World-Steel-in-Figures.pdf> (accessed on 19 October 2022).
36. Horii, K.; Tsutsumi, N.; Kitano, Y.; Kato, T. Processing and reusing technologies for steelmaking slag. *Nippon Steel Tech. Rep.* **2013**, *805*, 123–129.
37. Rashad, A.M. An overview on rheology, mechanical properties and durability of high-volume slag used as a cement replacement in paste, mortar and concrete. *Constr. Build. Mater.* **2018**, *187*, 89–117. [CrossRef]
38. Sakir, S.; Raman, S.N.; Safiuddin; Kaish, A.B.M.A.; Mutalib, A.A. Utilization of By-Products and Wastes as Supplementary Cementitious Materials in Structural Mortar for Sustainable Construction. *Sustainability* **2020**, *12*, 3888. [CrossRef]

39. Boukendakdji, O.; Kadri, E.-H.; Kenai, S. Effects of granulated blast furnace slag and superplasticizer type on the fresh properties and compressive strength of self-compacting concrete. *Cem. Concr. Compos.* **2012**, *34*, 583–590. [[CrossRef](#)]
40. Kuo, W.-T.; Chen, S.-H.; Wang, H.-Y.; Lin, J.-C. A study on the mechanical and electricity properties of cement mortar added with GGBFS and piezoelectric powder. *Constr. Build. Mater.* **2013**, *49*, 251–256. [[CrossRef](#)]
41. Onn, C.C.; Mo, K.H.; Radwan, M.K.H.; Liew, W.H.; Ng, C.G.; Yusoff, S. Strength, Carbon Footprint and Cost Considerations of Mortar Blends with High Volume Ground Granulated Blast Furnace Slag. *Sustainability* **2019**, *11*, 7194. [[CrossRef](#)]
42. Zhou, X.M.; Slater, J.R.; Wavell, S.E.; Oladiran, O. Effects of PFA and GGBS on Early-Ages Engineering Properties of Portland Cement Systems. *J. Adv. Concr. Technol.* **2012**, *10*, 74–85. [[CrossRef](#)]
43. Gholampour, A.; Ozbakkaloglu, T. Performance of sustainable concretes containing very high volume Class-F fly ash and ground granulated blast furnace slag. *J. Clean. Prod.* **2017**, *162*, 1407–1417. [[CrossRef](#)]
44. Bheel, N.; Abbasi, S.A.; Awoyera, P.; Olalusi, O.B.; Sohu, S.; Rondon, C.; Echeverría, A.M. Fresh and Hardened Properties of Concrete Incorporating Binary Blend of Metakaolin and Ground Granulated Blast Furnace Slag as Supplementary Cementitious Material. *Adv. Civ. Eng.* **2020**, *2020*, 8851030. [[CrossRef](#)]
45. Aghaeipour, A.; Madhkan, M. Effect of ground granulated blast furnace slag (GGBFS) on RCCP durability. *Constr. Build. Mater.* **2017**, *141*, 533–541. [[CrossRef](#)]
46. Wang, D.H.; Shi, C.J.; Farzadnia, N.; Shi, Z.G.; Jia, H.F.; Ou, Z.H. A review on use of limestone powder in cement-based materials: Mechanism, hydration and microstructures. *Constr. Build. Mater.* **2018**, *181*, 659–672. [[CrossRef](#)]
47. Courard, L.; Herfort, D.; Villagrán, Y. *Limestone Powder*; Springer: Berlin/Heidelberg, Germany, 2018; pp. 123–151.
48. Global Cement Staff. *Buzzi Unicem USA to Switch to Portland Limestone Cement Production by the End of 2022*; Global Cement: Epsom, UK, 2022.
49. Cement.org. *Portland-Limestone Cement and Sustainability*; Portland Cement Association: Washington, DC, USA, 2022.
50. Li, C.; Jiang, L.; Xu, N.; Jiang, S. Pore structure and permeability of concrete with high volume of limestone powder addition. *Powder Technol.* **2018**, *338*, 416–424. [[CrossRef](#)]
51. Kim, Y.-J.; van Leeuwen, R.; Cho, B.-Y.; Sriraman, V.; Torres, A. Evaluation of the Efficiency of Limestone Powder in Concrete and the Effects on the Environment. *Sustainability* **2018**, *10*, 550. [[CrossRef](#)]
52. Ramezani-pour, A.A.; Ghiasvand, E.; Nickseresht, I.; Mahdikhani, M.; Moodi, F. Influence of various amounts of limestone powder on performance of Portland limestone cement concretes. *Cem. Concr. Compos.* **2009**, *31*, 715–720. [[CrossRef](#)]
53. Liu, S.H.; Gao, Z.Y.; Rao, M.J. Study on the Ultra High Performance Concrete Containing Limestone Powder. *Adv. Mater. Res.* **2011**, *250–253*, 686–689. [[CrossRef](#)]
54. Liu, Z.; Deng, D.; De Schutter, G.; Yu, Z. The effect of  $MgSO_4$  on thaumasite formation. *Cem. Concr. Compos.* **2013**, *35*, 102–108. [[CrossRef](#)]
55. Yuan, B.; Yu, Q.L.; Brouwers, H.J.H. Assessing the chemical involvement of limestone powder in sodium carbonate activated slag. *Mater. Struct.* **2017**, *50*, 136. [[CrossRef](#)]
56. Sua-Iam, G.; Makul, N. Utilization of limestone powder to improve the properties of self-compacting concrete incorporating high volumes of untreated rice husk ash as fine aggregate. *Constr. Build. Mater.* **2013**, *38*, 455–464. [[CrossRef](#)]
57. Nepomuceno, M.; Oliveira, L.; Lopes, S. Methodology for mix design of the mortar phase of self-compacting concrete using different mineral additions in binary blends of powders. *Constr. Build. Mater.* **2012**, *26*, 317–326. [[CrossRef](#)]
58. Wang, Q.; Yang, J.; Chen, H. Long-term properties of concrete containing limestone powder. *Mater. Struct.* **2017**, *50*, 168. [[CrossRef](#)]
59. Lin, W.-T.; Cheng, A.; Černý, R. Effect of limestone powder on strength and permeability of cementitious mortars. *MATEC Web Conf.* **2020**, *322*, 01009. [[CrossRef](#)]
60. Black, L. Low clinker cement as a sustainable construction material. In *Sustainability of Construction Materials*; Elsevier: Amsterdam, The Netherlands, 2016; pp. 415–457.
61. Kumar, A.; Kumar, R.; Das, V.; Jhatial, A.A.; Ali, T.H. Assessing the structural efficiency and durability of burnt clay bricks incorporating fly ash and silica fume as additives. *Constr. Build. Mater.* **2021**, *310*, 125233. [[CrossRef](#)]
62. Nasr, M.S.; Hasan, Z.A.; Abed, M.K.; Dhahir, M.K.; Najim, W.N.; Shubbar, A.A.; Habeeb, Z.D. Utilization of High Volume Fraction of Binary Combinations of Supplementary Cementitious Materials in the Production of Reactive Powder Concrete. *Period. Polytech. Civ. Eng.* **2020**, *65*, 335–343. [[CrossRef](#)]
63. Wetzell, A.; Middendorf, B. Influence of silica fume on properties of fresh and hardened ultra-high performance concrete based on alkali-activated slag. *Cem. Concr. Compos.* **2019**, *100*, 53–59. [[CrossRef](#)]
64. Meddah, M.S.; Ismail, M.A.; El-Gamal, S.; Fitriani, H. Performances evaluation of binary concrete designed with silica fume and metakaolin. *Constr. Build. Mater.* **2018**, *166*, 400–412. [[CrossRef](#)]
65. Lin, W.-T.; Zhao, W.-Q.; Chang, Y.-H.; Yang, J.-S.; Cheng, A. The Effect of Incorporating Ultra-Fine Spherical Particles on Rheology and Engineering Properties of Commercial Ultra-High-Performance Grout. *Crystals* **2021**, *11*, 1040. [[CrossRef](#)]
66. Jeong, Y.; Kang, S.-H.; Kim, M.O.; Moon, J. Acceleration of cement hydration from supplementary cementitious materials: Performance comparison between silica fume and hydrophobic silica. *Cem. Concr. Compos.* **2020**, *112*, 103688. [[CrossRef](#)]
67. Gleize, P.; Müller, A.; Roman, H. Microstructural investigation of a silica fume–cement–lime mortar. *Cem. Concr. Compos.* **2003**, *25*, 171–175. [[CrossRef](#)]

68. Nili, M.; Ramezani pour, A.A.; Sobhani, J. Evaluation of the effects of silica fume and air-entrainment on deicer salt scaling resistance of concrete pavements: Microstructural study and modeling. *Constr. Build. Mater.* **2021**, *308*, 124972. [[CrossRef](#)]
69. Lü, Q.; Qiu, Q.; Zheng, J.; Wang, J.; Zeng, Q. Fractal dimension of concrete incorporating silica fume and its correlations to pore structure, strength and permeability. *Constr. Build. Mater.* **2019**, *228*, 116986. [[CrossRef](#)]
70. Keerio, M.A.; Abbasi, S.A.; Kumar, A.; Bheel, N.; Rehaman, K.U.; Tashfeen, M. Effect of Silica Fume as Cementitious Material and Waste Glass as Fine Aggregate Replacement Constituent on Selected Properties of Concrete. *Silicon* **2022**, *14*, 165–176. [[CrossRef](#)]
71. Elbasir, O.M.; Araba, A.; Miskeen, M.B.; Nser, S.; Fathi, N. Effect of Addition Silica Fume to the workability, Strength and Permeability of Concrete. *J. Pure Appl. Sci.* **2019**, *18*, 414–417.
72. Amudhavalli, N.K.; Mathew, J. Effect of Silica Fume on Strength and Durability Parameters of Concrete. *Int. J. Eng. Sci. Emerg. Technol.* **2012**, *3*, 2231–6604. Available online: <http://www.ijeset.com/media/4N5-IJESSET0202520.pdf> (accessed on 25 May 2022).
73. Hanumesh, B.M.; Varun, B.K.; Harish, B.A. The mechanical properties of concrete incorporating silica fume as partial replacement of cement. *Int. J. Emerg. Technol. Adv. Eng.* **2015**, *5*, 270.
74. Bonavetti, V.L.; Castellano, C.; Donza, H.; Rahhal, V.; Irassar, E.F. Cement with silica fume and granulated blast-furnace slag: Strength behavior and hydration. *Mater. Constr.* **2014**, *64*, e025. [[CrossRef](#)]
75. Vellaichamy, P.; Priyadharshini, S. Studies on Effect of Silica Fume on Workability and Strength of Concrete. *Int. Res. J. Multidiscip. Technovation* **2019**, *1*, 165–171. [[CrossRef](#)]
76. Tavares, L.R.C.; Junior, J.F.T.; Costa, L.M.; Bezerra, A.C.D.S.; Cetlin, P.R.; Aguilar, M.T.P. Influence of quartz powder and silica fume on the performance of Portland cement. *Sci. Rep.* **2020**, *10*, 21461. [[CrossRef](#)] [[PubMed](#)]
77. Kumar, S.; Kumar, B.; Swami, B.L.P. Effect of Metakaolin and Condensed Silica Fume on the Rheological and Structural Properties of Self-compacting Concrete. *Civ. Eng. Arch.* **2020**, *8*, 1057–1062. [[CrossRef](#)]
78. Sadrmomtazi, A.; Tahmouresi, B.; Khoshkbijari, R.K. Effect of fly ash and silica fume on transition zone, pore structure and permeability of concrete. *Mag. Concr. Res.* **2018**, *70*, 519–532. [[CrossRef](#)]
79. Shirdam, R.; Amini, M.; Bakhshi, N. Investigating the Effects of Copper Slag and Silica Fume on Durability, Strength, and Workability of Concrete. *Int. J. Environ. Res.* **2019**, *13*, 909–924. [[CrossRef](#)]
80. Gong, J.; Zhu, L.; Li, J.; Shi, D. Silica Fume and Nanosilica Effects on Mechanical and Shrinkage Properties of Foam Concrete for Structural Application. *Adv. Mater. Sci. Eng.* **2020**, *2020*, 3963089. [[CrossRef](#)]
81. Mohyiddeen, M.; Maya, T.M. Effect of Silica Fume on Concrete Containing Copper Slag as Fine Aggregate. *Int. J. Res. Advent Technol.* **2015**, *TASC-15*, 55–59.
82. Padavala, A.B.; Potharaju, M.; Kode, V.R. Mechanical properties of ternary blended mix concrete of fly ash and silica fume. *Mater. Today Proc.* **2021**, *43*, 2198–2202. [[CrossRef](#)]
83. BRMCA (British Ready Mix Concrete Association). *Cement Type/Early Age Properties—The Use of Low CO<sub>2</sub> Cements in Concrete Should not Restrict the Rate of Construction*; BRMCA (British Ready Mix Concrete Association): London, UK, 2011.
84. Maraghechi, H.; Avet, F.; Wong, H.; Kamyab, H.; Scrivener, K. Performance of Limestone Calcined Clay Cement (LC3) with various kaolinite contents with respect to chloride transport. *Mater. Struct.* **2018**, *51*, 125. [[CrossRef](#)]
85. Parra, P.A.Y.; Ganti, G.; Brecha, R.; Hare, B.; Schaeffer, M.; Fuentes, U. Global and Regional Coal Phase-Out Requirements of the Paris Agreement: Insights from the IPCC Special Report on 1.5 °C. 2019. Available online: [https://climateanalytics.org/media/report\\_coal\\_phase\\_out\\_2019.pdf](https://climateanalytics.org/media/report_coal_phase_out_2019.pdf) (accessed on 25 May 2022).
86. McCarthy, M.J.; Robl, T.; Csetenyi, L.J. Recovery, processing, and usage of wet-stored fly ash. In *Coal Combustion Products (CCP's)*; Elsevier: Amsterdam, The Netherlands, 2017; pp. 343–367.
87. Favier, A.; De Wolf, C.; Scrivener, K.; Habert, G. *A Sustainable Future for the European Cement and Concrete Industry: Technology Assessment for Full Decarbonisation of the Industry by 2050*; ETH Zurich: Zurich, Switzerland, 2018. [[CrossRef](#)]
88. Simonsen, A.M.T.; Solismaa, S.; Hansen, H.; Jensen, P.E. Evaluation of mine tailings' potential as supplementary cementitious materials based on chemical, mineralogical and physical characteristics. *Waste Manag.* **2020**, *102*, 710–721. [[CrossRef](#)]
89. Brown, T.J.; Idoine, N.E.; Wrighton, C.E.; Raycraft, E.R.; Hobbs, S.F.; Shaw, R.A.; Everett, P.; Deady, E.A.; Kresse, C. World Mineral Production 2015–2019. 2021. Available online: [https://www2.bgs.ac.uk/mineralsuk/download/world\\_statistics/2010s/WMP\\_2015\\_2019.pdf](https://www2.bgs.ac.uk/mineralsuk/download/world_statistics/2010s/WMP_2015_2019.pdf) (accessed on 25 May 2022).
90. Sun, W.; Ji, B.; Khoso, S.A.; Tang, H.; Liu, R.; Wang, L.; Hu, Y. An extensive review on restoration technologies for mining tailings. *Environ. Sci. Pollut. Res.* **2018**, *25*, 33911–33925. [[CrossRef](#)]
91. Yao, G.; Liu, Q.; Wang, J.; Wu, P.; Lyu, X. Effect of mechanical grinding on pozzolanic activity and hydration properties of siliceous gold ore tailings. *J. Clean. Prod.* **2019**, *217*, 12–21. [[CrossRef](#)]
92. Ye, J.; Zhang, W.; Shi, D. Properties of an aged geopolymer synthesized from calcined ore-dressing tailing of bauxite and slag. *Cem. Concr. Res.* **2017**, *100*, 23–31. [[CrossRef](#)]
93. Ghazi, A.B.; Jamshidi-Zanjani, A.; Nejati, H. Utilization of copper mine tailings as a partial substitute for cement in concrete construction. *Constr. Build. Mater.* **2022**, *317*, 125921. [[CrossRef](#)]
94. Thomas, B.S.; Damare, A.; Gupta, R. Strength and durability characteristics of copper tailing concrete. *Constr. Build. Mater.* **2013**, *48*, 894–900. [[CrossRef](#)]
95. Kiventerä, J.; Lancellotti, I.; Catauro, M.; Poggetto, F.D.; Leonelli, C.; Illikainen, M. Alkali activation as new option for gold mine tailings inertization. *J. Clean. Prod.* **2018**, *187*, 76–84. [[CrossRef](#)]

96. Sigvardsen, N.M.; Nielsen, M.R.; Potier, C.; Ottosen, L.M.; Jensen, P.E. Utilization of Mine Tailings As Partial Cement Replacement. *Mod. Environ. Sci. Eng.* **2018**, *4*, 365–374. [[CrossRef](#)]
97. Wang, Q.; Yao, G.; Zhu, X.; Wang, J.; Wu, P.; Lyu, X. Preparation of Portland Cement with Gold Ore Tailings. *Adv. Mater. Sci. Eng.* **2019**, *2019*, 1324065. [[CrossRef](#)]
98. Bezerra, C.G.; Rocha, C.A.A.; de Siqueira, I.S.; Filho, R.D.T. Feasibility of iron-rich ore tailing as supplementary cementitious material in cement pastes. *Constr. Build. Mater.* **2021**, *303*, 124496. [[CrossRef](#)]
99. Shettima, A.U.; Hussin, M.W.; Ahmad, Y.; Mirza, J. Evaluation of iron ore tailings as replacement for fine aggregate in concrete. *Constr. Build. Mater.* **2016**, *120*, 72–79. [[CrossRef](#)]
100. Ling, G.; Shui, Z.; Gao, X.; Sun, T.; Yu, R.; Li, X. Utilizing Iron Ore Tailing as Cementitious Material for Eco-Friendly Design of Ultra-High Performance Concrete (UHPC). *Materials* **2021**, *14*, 1829. [[CrossRef](#)] [[PubMed](#)]
101. Zheng, K.; Zhou, J.; Gbozee, M. Influences of phosphate tailings on hydration and properties of Portland cement. *Constr. Build. Mater.* **2015**, *98*, 593–601. [[CrossRef](#)]
102. Pyo, S.; Tafesse, M.; Kim, B.-J.; Kim, H.-K. Effects of quartz-based mine tailings on characteristics and leaching behavior of ultra-high performance concrete. *Constr. Build. Mater.* **2018**, *166*, 110–117. [[CrossRef](#)]
103. Janković, K.; Šušić, N.; Stojanović, M.; Bojović, D.; Lončar, L. The influence of tailings and cement type on durability properties of self-compacting concrete. *Teh. Vjesn.* **2017**, *24*, 957–962. [[CrossRef](#)]
104. Zhao, S.; Fan, J.; Sun, W. Utilization of iron ore tailings as fine aggregate in ultra-high performance concrete. *Constr. Build. Mater.* **2014**, *50*, 540–548. [[CrossRef](#)]
105. Mao, S.; Zhang, Q. Mineralogical Characteristics of Phosphate Tailings for Comprehensive Utilization. *Adv. Civ. Eng.* **2021**, *2021*, 5529021. [[CrossRef](#)]
106. Ince, C. Reusing gold-mine tailings in cement mortars: Mechanical properties and socio-economic developments for the Lefke-Xeros area of Cyprus. *J. Clean. Prod.* **2019**, *238*, 117871. [[CrossRef](#)]
107. Galvão, J.L.B.; Andrade, H.D.; Brigolini, G.J.; Peixoto, R.A.F.; Mendes, J.C. Reuse of iron ore tailings from tailings dams as pigment for sustainable paints. *J. Clean. Prod.* **2018**, *200*, 412–422. [[CrossRef](#)]
108. Onuaguluchi, O.; Eren, Ö. Recycling of copper tailings as an additive in cement mortars. *Constr. Build. Mater.* **2012**, *37*, 723–727. [[CrossRef](#)]
109. Esmaeili, J.; Aslani, H. Use of copper mine tailing in concrete: Strength characteristics and durability performance. *J. Mater. Cycles Waste Manag.* **2019**, *21*, 729–741. [[CrossRef](#)]
110. Vargas, F.; Lopez, M.; Rigamonti, L. Environmental impacts evaluation of treated copper tailings as supplementary cementitious materials. *Resour. Conserv. Recycl.* **2020**, *160*, 104890. [[CrossRef](#)]
111. Onuaguluchi, O.; Eren, Ö. Reusing copper tailings in concrete: Corrosion performance and socioeconomic implications for the Lefke-Xeros area of Cyprus. *J. Clean. Prod.* **2016**, *112*, 420–429. [[CrossRef](#)]
112. Cheng, Y.; Huang, F.; Li, W.; Liu, R.; Li, G.; Wei, J. Test research on the effects of mechanochemically activated iron tailings on the compressive strength of concrete. *Constr. Build. Mater.* **2016**, *118*, 164–170. [[CrossRef](#)]
113. Xiong, C.; Li, W.; Jiang, L.; Wang, W.; Guo, Q. Use of grounded iron ore tailings (GIOTs) and BaCO<sub>3</sub> to improve sulfate resistance of pastes. *Constr. Build. Mater.* **2017**, *150*, 66–76. [[CrossRef](#)]
114. Wang, Q.; Li, J.; Zhu, X.; Yao, G.; Wu, P.; Wang, Z.; Lyu, X.; Hu, S.; Qiu, J.; Chen, P.; et al. Approach to the management of gold ore tailings via its application in cement production. *J. Clean. Prod.* **2020**, *269*, 122303. [[CrossRef](#)]
115. Luo, L.; Zhang, Y.; Bao, S.; Chen, T. Utilization of Iron Ore Tailings as Raw Material for Portland Cement Clinker Production. *Adv. Mater. Sci. Eng.* **2016**, *2016*, 1596047. [[CrossRef](#)]
116. Young, G.; Yang, M. Preparation and characterization of Portland cement clinker from iron ore tailings. *Constr. Build. Mater.* **2019**, *197*, 152–156. [[CrossRef](#)]
117. de Magalhães, L.F.; Morais, I.D.S.; Lara, L.F.D.S.; de Resende, D.S.; Menezes, R.M.R.O.; Aguilar, M.T.P.; Bezerra, A.C.D.S. Iron Ore Tailing as Addition to Partial Replacement of Portland Cement. *Mater. Sci. Forum* **2018**, *930*, 125–130. [[CrossRef](#)]
118. de Magalhães, L.F.; França, S.; Oliveira, M.D.S.; Peixoto, R.A.F.; Bessa, S.A.L.; Bezerra, A.C.D.S. Iron ore tailings as a supplementary cementitious material in the production of pigmented cements. *J. Clean. Prod.* **2020**, *274*, 123260. [[CrossRef](#)]
119. Agrawal, Y.; Gupta, T.; Chaudhary, S. Effect of mechanically treated and untreated zinc tailing waste as cement substitute in concrete production: An experimental and statistical analysis. *Environ. Sci. Pollut. Res.* **2022**, *29*, 28598–28623. [[CrossRef](#)] [[PubMed](#)]
120. Lim, Y.C.; Chen, C.-F.; Chen, C.-W.; Dong, C.-D. Application of Basic Oxygen Furnace Slag in Increased Utilization of Dredged Harbor Sediment. *J. Sustain. Metall.* **2021**, *7*, 704–717. [[CrossRef](#)]
121. Wang, G.; Wang, Y.; Gao, Z. Use of steel slag as a granular material: Volume expansion prediction and usability criteria. *J. Hazard. Mater.* **2010**, *184*, 555–560. [[CrossRef](#)] [[PubMed](#)]
122. Mailar, G.; Sreedhara, B.M.; Manu, D.S.; Hiremath, P.; Jayakesh, K. Investigation of concrete produced using recycled aluminium dross for hot weather concreting conditions. *Resour. Technol.* **2016**, *2*, 68–80. [[CrossRef](#)]
123. Dai, C. *Development of Aluminium Dross-Based Material for Engineering Applications*; Worcester Polytechnic Institute: Worcester, MA, USA, 2012.
124. Shen, H.; Liu, B.; Ekberg, C.; Zhang, S. Harmless disposal and resource utilization for secondary aluminum dross: A review. *Sci. Total Environ.* **2020**, *760*, 143968. [[CrossRef](#)]

125. Mahinroosta, M.; Allahverdi, A. Hazardous aluminum dross characterization and recycling strategies: A critical review. *J. Environ. Manag.* **2018**, *223*, 452–468. [[CrossRef](#)]
126. Environmental Protection Agency. Waste Classification List of Waste & Determining if Waste is Hazardous or Non-hazardous. 2018. Available online: [Epa.ie/publications/monitoring--assessment/waste/2019--FULL-template.pdf](https://epa.ie/publications/monitoring--assessment/waste/2019--FULL-template.pdf) (accessed on 25 May 2022).
127. Adeosun, S.O. Physical and Mechanical Properties of Aluminum Dross. *Adv. Mater.* **2014**, *3*, 6. [[CrossRef](#)]
128. Arimanwa, J.I.; Onwuka, D.O.; Arimanwa, M.C.; Onwuka, U.S. Prediction of the Compressive Strength of Aluminum Waste–Cement Concrete Using Scheffe’s Theory. *J. Mater. Civ. Eng.* **2012**, *24*, 177–183. [[CrossRef](#)]
129. Elinwa, A.; Mbadike, E. The Use of Aluminum Waste for Concrete Production. *J. Asian Arch. Build. Eng.* **2011**, *10*, 217–220. [[CrossRef](#)]
130. Javali, S.; Chandrashekar, A.R.; Naganna, S.R.; Manu, D.S.; Hiremath, P.; Preethi, H.G.; Kumar, N.V. Eco-concrete for sustainability: Utilizing aluminium dross and iron slag as partial replacement materials. *Clean Technol. Environ. Policy* **2017**, *19*, 2291–2304. [[CrossRef](#)]
131. Reddy, M.S.; Neeraja, D. Mechanical and durability aspects of concrete incorporating secondary aluminium slag. *Resour. Technol.* **2016**, *2*, 225–232. [[CrossRef](#)]
132. Panditharadhya, B.J.; Sampath, V.; Mulangi, R.H.; Shankar, A.U.R. Mechanical properties of pavement quality concrete with secondary aluminium dross as partial replacement for ordinary portland cement. *IOP Conf. Ser. Mater. Sci. Eng.* **2018**, *431*, 032011. [[CrossRef](#)]
133. Piemonti, A.; Conforti, A.; Cominoli, L.; Sorlini, S.; Luciano, A.; Plizzari, G. Use of Iron and Steel Slags in Concrete: State of the Art and Future Perspectives. *Sustainability* **2021**, *13*, 556. [[CrossRef](#)]
134. Rađenović, A.; Malina, J.; Sofilić, T. Characterization of Ladle Furnace Slag from Carbon Steel Production as a Potential Adsorbent. *Adv. Mater. Sci. Eng.* **2013**, *2013*, 198240. [[CrossRef](#)]
135. Reddy, A.S.; Pradhan, R.; Chandra, S. Utilization of Basic Oxygen Furnace (BOF) slag in the production of a hydraulic cement binder. *Int. J. Miner. Process.* **2006**, *79*, 98–105. [[CrossRef](#)]
136. EÖzbay, E.; Erdemir, M.; Durmuş, H.İ. Utilization and efficiency of ground granulated blast furnace slag on concrete properties—A review. *Constr. Build. Mater.* **2016**, *105*, 423–434. [[CrossRef](#)]
137. Muhmood, L.; Vitta, S.; Venkateswaran, D. Cementitious and pozzolanic behavior of electric arc furnace steel slags. *Cem. Concr. Res.* **2009**, *39*, 102–109. [[CrossRef](#)]
138. Khan, K.; Amin, M.N. Influence of fineness of volcanic ash and its blends with quarry dust and slag on compressive strength of mortar under different curing temperatures. *Constr. Build. Mater.* **2017**, *154*, 514–528. [[CrossRef](#)]
139. Parron-Rubio, M.E.; Perez-García, F.; Gonzalez-Herrera, A.; Rubio-Cintas, M.D. Concrete Properties Comparison When Substituting a 25% Cement with Slag from Different Provenances. *Materials* **2018**, *11*, 1029. [[CrossRef](#)]
140. Choi, S.-J.; Kim, Y.-U.; Oh, T.-G.; Cho, B.-S. Compressive Strength, Chloride Ion Penetrability, and Carbonation Characteristic of Concrete with Mixed Slag Aggregate. *Materials* **2020**, *13*, 940. [[CrossRef](#)]
141. Lee, J.-Y.; Choi, J.-S.; Yuan, T.-F.; Yoon, Y.-S.; Mitchell, D. Comparing Properties of Concrete Containing Electric Arc Furnace Slag and Granulated Blast Furnace Slag. *Materials* **2019**, *12*, 1371. [[CrossRef](#)] [[PubMed](#)]
142. Lun, Y.; Zhou, M.; Cai, X.; Xu, F. Methods for improving volume stability of steel slag as fine aggregate. *J. Wuhan Univ. Technol. Sci. Ed.* **2008**, *23*, 737–742. [[CrossRef](#)]
143. Quadir, M. Flexural Strength of Concrete by Partial Replacement of Sand with Basic Oxygen Furnace Slag. *Res. Rev. J. Eng. Technol.* **2018**, *7*, 8–17.
144. Coppola, L.; Buoso, A.; Coffetti, D.; Kara, P.; Lorenzi, S. Electric arc furnace granulated slag for sustainable concrete. *Constr. Build. Mater.* **2016**, *123*, 115–119. [[CrossRef](#)]
145. Sekaran, A.; Palaniswamy, M.; Balaraju, S. A Study on Suitability of EAF Oxidizing Slag in Concrete: An Eco-Friendly and Sustainable Replacement for Natural Coarse Aggregate. *Sci. World J.* **2015**, *2015*, 469376. [[CrossRef](#)]
146. Jexembayeva, A.; Salem, T.; Jiao, P.; Hou, B.; Niyazbekova, R. Blended Cement Mixed with Basic Oxygen Steelmaking Slag (BOF) as an Alternative Green Building Material. *Materials* **2020**, *13*, 3062. [[CrossRef](#)]
147. Amin, M.N.; Khan, K.; Saleem, M.U.; Khurram, N.; Niazi, M.U.K. Influence of Mechanically Activated Electric Arc Furnace Slag on Compressive Strength of Mortars Incorporating Curing Moisture and Temperature Effects. *Sustainability* **2017**, *9*, 1178. [[CrossRef](#)]
148. Roslan, N.H.; Ismail, M.; Abdul-Majid, Z.; Ghoreishiamiri, S.; Muhammad, B. Performance of steel slag and steel sludge in concrete. *Constr. Build. Mater.* **2016**, *104*, 16–24. [[CrossRef](#)]
149. Roslan, N.H.; Ismail, M.; Khalid, N.H.A.; Muhammad, B. Properties of concrete containing electric arc furnace steel slag and steel sludge. *J. Build. Eng.* **2020**, *28*, 101060. [[CrossRef](#)]
150. Shi, Y.; Chen, H.; Wang, J.; Feng, Q. Preliminary investigation on the pozzolanic activity of superfine steel slag. *Constr. Build. Mater.* **2015**, *82*, 227–234. [[CrossRef](#)]
151. Chowdhury, S.; Mishra, M.; Suganya, O. The incorporation of wood waste ash as a partial cement replacement material for making structural grade concrete: An overview. *Ain Shams Eng. J.* **2015**, *6*, 429–437. [[CrossRef](#)]
152. Cheah, C.B.; Ramli, M. The implementation of wood waste ash as a partial cement replacement material in the production of structural grade concrete and mortar: An overview. *Resour. Conserv. Recycl.* **2011**, *55*, 669–685. [[CrossRef](#)]

153. Lakusic, S. Wood biomass ash as a raw material in concrete industry. *J. Croat. Assoc. Civ. Eng.* **2019**, *71*, 505–514. [[CrossRef](#)]
154. Vu, V.-A.; Cloutier, A.; Bissonnette, B.; Blanchet, P.; Duchesne, J. The Effect of Wood Ash as a Partial Cement Replacement Material for Making Wood-Cement Panels. *Materials* **2019**, *12*, 2766. [[CrossRef](#)]
155. Wang, S.; Baxter, L.; Fonseca, F. Biomass fly ash in concrete: SEM, EDX and ESEM analysis. *Fuel* **2008**, *87*, 372–379. [[CrossRef](#)]
156. Etiégni, L.; Campbell, A. Physical and chemical characteristics of wood ash. *Bioresour. Technol.* **1991**, *37*, 173–178. [[CrossRef](#)]
157. Vassilev, S.V.; Baxter, D.; Andersen, L.K.; Vassileva, C.G. An overview of the chemical composition of biomass. *Fuel* **2010**, *89*, 913–933. [[CrossRef](#)]
158. Awolusi, T.F.; Sojobi, A.O.; Oguntayo, D.O.; Akinkulolere, O.O.; Orogbade, B. Effects of calcined clay, sawdust ash and chemical admixtures on Strength and Properties of concrete for pavement and flooring applications using Taguchi approach. *Case Stud. Constr. Mater.* **2021**, *15*, e00568. [[CrossRef](#)]
159. Raza, M.S.; Rai, K.; Kumar, D.; Ali, M. Experimental Study of Physical, Fresh-State and Strength Parameters of Concrete incorporating Wood Waste Ash as a Cementitious Material. *J. Mater. Eng. Struct.* **2020**, *7*, 267–276.
160. Bhat, J.A. Mechanical behaviour of self compacting concrete: Effect of wood ash and coal ash as partial cement replacement. *Mater. Today Proc.* **2021**, *42*, 1470–1476. [[CrossRef](#)]
161. Keppert, M.; Davidová, V.; Doušová, B.; Scheinherrová, L.; Reiterman, P. Recycling of fresh concrete slurry waste as supplementary cementing material: Characterization, application and leaching of selected elements. *Constr. Build. Mater.* **2021**, *300*, 124061. [[CrossRef](#)]
162. Schneider, M. The cement industry on the way to a low-carbon future. *Cem. Concr. Res.* **2019**, *124*, 105792. [[CrossRef](#)]
163. Xuan, D.; Zhan, B.; Poon, C.S.; Zheng, W. Innovative reuse of concrete slurry waste from ready-mixed concrete plants in construction products. *J. Hazard. Mater.* **2016**, *312*, 65–72. [[CrossRef](#)] [[PubMed](#)]
164. Kesikidou, F.; Konopisi, S.; Anastasiou, E.K. Influence of Concrete Sludge Addition in the Properties of Alkali-Activated and Non-Alkali-Activated Fly Ash-Based Mortars. *Adv. Civ. Eng.* **2021**, *2021*, 5534002. [[CrossRef](#)]
165. Wang, R.; Zhang, Y.X. Recycling fresh concrete waste: A review. *Struct. Concr.* **2018**, *19*, 1939–1955. [[CrossRef](#)]
166. Kaliyavaradhan, S.K.; Ling, T.-C.; Mo, K.H. Valorization of waste powders from cement-concrete life cycle: A pathway to circular future. *J. Clean. Prod.* **2020**, *268*, 122358. [[CrossRef](#)]
167. Hossain, U.; Xuan, D.; Poon, C.S. Sustainable management and utilisation of concrete slurry waste: A case study in Hong Kong. *Waste Manag.* **2017**, *61*, 397–404. [[CrossRef](#)]
168. Tang, P.; Xuan, D.; Poon, C.S.; Tsang, D.C. Valorization of concrete slurry waste (CSW) and fine incineration bottom ash (IBA) into cold bonded lightweight aggregates (CBLAs): Feasibility and influence of binder types. *J. Hazard. Mater.* **2019**, *368*, 689–697. [[CrossRef](#)]
169. He, X.; Zheng, Z.; Ma, M.; Su, Y.; Yang, J.; Tan, H.; Wang, Y.; Strnadel, B. New treatment technology: The use of wet-milling concrete slurry waste to substitute cement. *J. Clean. Prod.* **2020**, *242*, 118347. [[CrossRef](#)]
170. Kou, S.-C.; Zhan, B.-J.; Poon, C.-S. Properties of partition wall blocks prepared with fresh concrete wastes. *Constr. Build. Mater.* **2012**, *36*, 566–571. [[CrossRef](#)]
171. Xi, Y.; Anastasiou, E.; Karozou, A.; Silvestri, S. Fresh and hardened properties of cement mortars using marble sludge fines and cement sludge fines. *Constr. Build. Mater.* **2019**, *220*, 142–148. [[CrossRef](#)]
172. Papí, J.A.F. Recycling of fresh concrete exceeding and wash water in concrete mixing plants. *Mater. Constr.* **2014**, *64*, e004. [[CrossRef](#)]
173. Chen, X.; Li, Y.; Bai, H.; Ma, L. Utilization of Recycled Concrete Powder in Cement Composite: Strength, Microstructure and Hydration Characteristics. *J. Renew. Mater.* **2021**, *9*, 2189–2208. [[CrossRef](#)]
174. Horsakulthai, V. Effect of recycled concrete powder on strength, electrical resistivity, and water absorption of self-compacting mortars. *Case Stud. Constr. Mater.* **2021**, *15*, e00725. [[CrossRef](#)]
175. Ren, P.; Li, B.; Yu, J.-G.; Ling, T.-C. Utilization of recycled concrete fines and powders to produce alkali-activated slag concrete blocks. *J. Clean. Prod.* **2020**, *267*, 122115. [[CrossRef](#)]
176. Rakhimova, N.R.; Rakhimov, R.Z. Hydrated Portland cement as an admixture to alkali-activated slag cement. *Adv. Cem. Res.* **2015**, *27*, 107–117. [[CrossRef](#)]
177. Kim, Y.J.; Choi, Y.W. Utilization of waste concrete powder as a substitution material for cement. *Constr. Build. Mater.* **2012**, *30*, 500–504. [[CrossRef](#)]
178. Zhu, P.; Mao, X.; Qu, W. Investigation of recycled powder as supplementary cementitious material. *Mag. Concr. Res.* **2019**, *71*, 1312–1324. [[CrossRef](#)]
179. Sun, C.; Chen, L.; Xiao, J.; Singh, A.; Zeng, J. Compound utilization of construction and industrial waste as cementitious recycled powder in mortar. *Resour. Conserv. Recycl.* **2021**, *170*, 105561. [[CrossRef](#)]
180. Kalinowska-Wichrowska, K.; Kosior-Kazberuk, M.; Pawluczuk, E. The Properties of Composites with Recycled Cement Mortar Used as a Supplementary Cementitious Material. *Materials* **2019**, *13*, 64. [[CrossRef](#)]
181. Sun, Z.; Liu, F.; Tong, T.; Qi, C.; Yu, Q. Hydration of Concrete Containing Hybrid Recycled Demolition Powders. *J. Mater. Civ. Eng.* **2017**, *29*, 04017037. [[CrossRef](#)]
182. Qing-Hua, C.; Tagnit-Hamou, A.; Sarkar, S.L. Strength and Microstructural Properties of Water Glass Activated Slag. *MRS Proc.* **1991**, *245*, 49. [[CrossRef](#)]

183. ASTM C989-06; Standard Specification for Ground Granulated Blast-Furnace Slag for Use in Concrete and Mortars. ASTM: West Conshohocken, PA, USA, 2006.
184. EN 15167-1:2008; Ground Granulated Blast Furnace Slag for Use in Concrete, Mortar and Grout—Part 1: Definitions, Specifications and Conformity Criteria. iTeh, Inc.: Newark, DE, USA, 2008. Available online: <https://www.en-standard.eu/une-en-15167-1-2008-ground-granulated-blast-furnace-slag-for-use-in-concrete-mortar-and-grout-part-1-definitions-specifications-and-conformity-criteria/> (accessed on 17 September 2022).
185. IS 15388; Silica Fume—Specification. Bureau of Indian Standards: New Delhi, India. Bureau of Indian Standards: New Delhi, India, 2003. Available online: [https://infostore.saiglobal.com/en-gb/standards/bis-is-15388-2003-r2017--183786\\_saig\\_bis\\_bis\\_442818/](https://infostore.saiglobal.com/en-gb/standards/bis-is-15388-2003-r2017--183786_saig_bis_bis_442818/) (accessed on 17 September 2022).
186. EN 13263-1:2005+A1:2009; Silica Fume for Concrete—Part 1: Definitions, Requirements and Conformity Criteria. iTeh, Inc.: Newark, DE, USA, 2009.
187. ASTM C1240-20; Standard Specification for Silica Fume Used in Cementitious Mixtures. ASTM: West Conshohocken, PA, USA, 2020. Available online: <https://www.astm.org/c1240-20.html> (accessed on 17 September 2022).
188. ASTM C1797-17; Standard Specification for Ground Calcium Carbonate and Aggregate Mineral Fillers for Use in Hydraulic Cement Concrete. ASTM: West Conshohocken, PA, USA, 2017. Available online: <https://www.astm.org/c1797-17.html> (accessed on 17 September 2022).
189. Nedeljković, M.; Visser, J.; Šavija, B.; Valcke, S.; Schlangen, E. Use of fine recycled concrete aggregates in concrete: A critical review. *J. Build. Eng.* **2021**, *38*, 102196. [[CrossRef](#)]
190. Snellings, R. Assessing, Understanding and Unlocking Supplementary Cementitious Materials. *RILEM Tech. Lett.* **2016**, *1*, 50–55. [[CrossRef](#)]
191. Tangchirapat, W.; Tangpagasit, J.; Waew-kum, S.; Jaturapitakkul, C. A new pozzolanic material from palm oil fuel ash. *KMUTT Res. Dev. J.* **2003**, *26*, 459–473.
192. Hou, P.-K.; Kawashima, S.; Wang, K.-J.; Corr, D.J.; Qian, J.-S.; Shah, S.P. Effects of colloidal nanosilica on rheological and mechanical properties of fly ash–cement mortar. *Cem. Concr. Compos.* **2013**, *35*, 12–22. [[CrossRef](#)]
193. Lothenbach, B.; Le Saout, G.; Ben Haha, M.; Figi, R.; Wieland, E. Hydration of a low-alkali CEM III/B–SiO<sub>2</sub> cement (LAC). *Cem. Concr. Res.* **2012**, *42*, 410–423. [[CrossRef](#)]
194. Yu, R.; Spiesz, P.; Brouwers, H.J.H. Effect of nano-silica on the hydration and microstructure development of Ultra-High Performance Concrete (UHPC) with a low binder amount. *Constr. Build. Mater.* **2014**, *65*, 140–150. [[CrossRef](#)]
195. Askarnejad, A.; Pourkhorshidi, A.R.; Parhizkar, T. Evaluation the pozzolanic reactivity of sonochemically fabricated nano natural pozzolan. *Ultrason. Sonochem.* **2012**, *19*, 119–124. [[CrossRef](#)]
196. Farzadnia, N.; Ali, A.A.A.; Demirboga, R. Characterization of high strength mortars with nano alumina at elevated temperatures. *Cem. Concr. Res.* **2013**, *54*, 43–54. [[CrossRef](#)]
197. Kiventerä, J.; Perumal, P.; Yliniemi, J.; Illikainen, M. Mine tailings as a raw material in alkali activation: A review. *Int. J. Miner. Met. Mater.* **2020**, *27*, 1009–1020. [[CrossRef](#)]
198. Adesanya, E.; Ohenoja, K.; Yliniemi, J.; Illikainen, M. Mechanical transformation of phyllite mineralogy toward its use as alkali-activated binder precursor. *Miner. Eng.* **2020**, *145*, 106093. [[CrossRef](#)]
199. Yao, G.; Wang, Q.; Wang, Z.; Wang, J.; Lyu, X. Activation of hydration properties of iron ore tailings and their application as supplementary cementitious materials in cement. *Powder Technol.* **2020**, *360*, 863–871. [[CrossRef](#)]
200. Rodriguez, E.D.; Bernal, S.A.; Provis, J.L.; Payá, J.; Monzó, J.M.; Borrachero, M.V. Structure of Portland Cement Pastes Blended with Sonicated Silica Fume. *J. Mater. Civ. Eng.* **2012**, *24*, 1295–1304. [[CrossRef](#)]
201. Kawashima, S.; Seo, J.-W.T.; Corr, D.; Hersam, M.C.; Shah, S.P. Dispersion of CaCO<sub>3</sub> nanoparticles by sonication and surfactant treatment for application in fly ash–cement systems. *Mater. Struct.* **2014**, *47*, 1011–1023. [[CrossRef](#)]
202. Yanguatin, H.; Ramírez, J.H.; Tironi, A.; Tobón, J. Effect of thermal treatment on pozzolanic activity of excavated waste clays. *Constr. Build. Mater.* **2019**, *211*, 814–823. [[CrossRef](#)]
203. Shen, J.; Liu, X.; Zhu, S.; Zhang, H.; Tan, J. Effects of calcination parameters on the silica phase of original and leached rice husk ash. *Mater. Lett.* **2011**, *65*, 1179–1183. [[CrossRef](#)]
204. Perumal, P.; Niu, H.; Kiventerä, J.; Kinnunen, P.; Illikainen, M. Upcycling of mechanically treated silicate mine tailings as alkali activated binders. *Miner. Eng.* **2020**, *158*, 106587. [[CrossRef](#)]
205. Perumal, P.; Piekkari, K.; Sreenivasan, H.; Kinnunen, P.; Illikainen, M. One-part geopolymers from mining residues—Effect of thermal treatment on three different tailings. *Miner. Eng.* **2019**, *144*, 106026. [[CrossRef](#)]
206. Guo, Z.; Feng, Q.; Wang, W.; Huang, Y.; Deng, J.; Xu, Z. Study on Flotation Tailings of Kaolinite-type Pyrite when Used as Cement Admixture and Concrete Admixture. *Procedia Environ. Sci.* **2016**, *31*, 644–652. [[CrossRef](#)]
207. Wong, R.; Gillott, J.; Law, S.; Thomas, M.; Poon, C. Calcined oil sands fine tailings as a supplementary cementing material for concrete. *Cem. Concr. Res.* **2004**, *34*, 1235–1242. [[CrossRef](#)]
208. Ghorbel, H.; Samet, B. Effect of iron on pozzolanic activity of kaolin. *Constr. Build. Mater.* **2013**, *44*, 185–191. [[CrossRef](#)]
209. Soro, N.S. *Influence des Ions fer sur les Transformations Thermiques de la Kaolinite*; University of Limoges: Limoges, France, 2003.
210. Taylor-Lange, S.C.; Rajabali, F.; Holsomback, N.A.; Riding, K.; Juenger, M.C. The effect of zinc oxide additions on the performance of calcined sodium montmorillonite and illite shale supplementary cementitious materials. *Cem. Concr. Compos.* **2014**, *53*, 127–135. [[CrossRef](#)]

211. Vayghan, A.G.; Khaloo, A.; Rajabipour, F. The effects of a hydrochloric acid pre-treatment on the physicochemical properties and pozzolanic performance of rice husk ash. *Cem. Concr. Compos.* **2013**, *39*, 131–140. [[CrossRef](#)]
212. Ataie, F.F.; Riding, K.A. Thermochemical Pretreatments for Agricultural Residue Ash Production for Concrete. *J. Mater. Civ. Eng.* **2013**, *25*, 1703–1711. [[CrossRef](#)]
213. Sicakova, A.; Kovac, M. Technological characterisation of selected mineral additives. *IOP Conf. Ser. Mater. Sci. Eng.* **2018**, *385*, 012048. [[CrossRef](#)]
214. *BS EN 196-1:2005*; Methods of Testing Cement Part 5: Pozzolanicity Test for Pozzolanic Cement. BSI: London, UK, 2005.
215. *NF P18-513*; Additions Pour Béton Hydraulique Métakaolin Spécifications et Critères de Conformité. Association Francaise de Normalisation: Toulouse, France, 2012.
216. Ali, H.A.; Xuan, D.; Poon, C.S. Assessment of long-term reactivity of initially lowly-reactive solid wastes as supplementary cementitious materials (SCMs). *Constr. Build. Mater.* **2020**, *232*, 117192. [[CrossRef](#)]
217. Li, X.; Snellings, R.; Antoni, M.; Alderete, N.M.; Ben Haha, M.; Bishnoi, S.; Cizer, Ö.; Cyr, M.; De Weerd, K.; Dhandapani, Y.; et al. Reactivity tests for supplementary cementitious materials: RILEM TC 267-TRM phase 1. *Mater. Struct.* **2018**, *51*, 151. [[CrossRef](#)]
218. Avet, F.; Snellings, R.; Diaz, A.A.; Ben Haha, M.; Scrivener, K. Development of a new rapid, relevant and reliable ( $R^3$ ) test method to evaluate the pozzolanic reactivity of calcined kaolinitic clays. *Cem. Concr. Res.* **2016**, *85*, 1–11. [[CrossRef](#)]
219. *ASTM C1897*; Standard Test Methods for Measuring the Reactivity of Supplementary Cementitious Materials by Isothermal Calorimetry and Bound Water Measurements. ASTM: West Conshohocken, PA, USA, 2020.
220. *ASTM C1608-17*; Standard Test Method for Chemical Shrinkage of Hydraulic Cement Paste. ASTM: West Conshohocken, PA, USA, 2017. Available online: <http://www.astm.org/cgi-bin/resolver.cgi?C1608> (accessed on 17 September 2022).
221. Scrivener, K.; Snellings, R.; Lothenbach, B. (Eds.) *A Practical Guide to Microstructural Analysis of Cementitious Materials*; CRC Press: Boca Raton, FL, USA, 2018.
222. Suraneni, P.; Weiss, J. Examining the pozzolanicity of supplementary cementitious materials using isothermal calorimetry and thermogravimetric analysis. *Cem. Concr. Compos.* **2017**, *83*, 273–278. [[CrossRef](#)]
223. *IS 1727-1967*; Methods of Test for Pozzolanic Materials. Bureau of Indian Standards: New Delhi, India, 2004.
224. Parashar, A.; Bishnoi, S. A comparison of test methods to assess the strength potential of plain and blended supplementary cementitious materials. *Constr. Build. Mater.* **2020**, *256*, 119292. [[CrossRef](#)]
225. *ASTM C311/C311M*; Standard Test Methods for Sampling and Testing Fly Ash or Natural Pozzolans for Use in Portland-Cement Concrete. ASTM: West Conshohocken, PA, USA, 2022. Available online: [https://www.astm.org/c0311\\_c0311m-22.html](https://www.astm.org/c0311_c0311m-22.html) (accessed on 17 September 2022).
226. Ramanathan, S.; Kasaniya, M.; Tuen, M.; Thomas, M.D.; Suraneni, P. Linking reactivity test outputs to properties of cementitious pastes made with supplementary cementitious materials. *Cem. Concr. Compos.* **2020**, *114*, 103742. [[CrossRef](#)]
227. Suraneni, P.; Burris, L.; Shearer, C.R.; Hooton, R.D. ASTM C618 Fly Ash Specification: Comparison with Other Specifications, Shortcomings, and Solutions. *ACI Mater. J.* **2021**, *118*, 157–167. [[CrossRef](#)]
228. Wang, Y.; Burris, L.; Shearer, C.R.; Hooton, D.; Suraneni, P. Strength activity index and bulk resistivity index modifications that differentiate inert and reactive materials. *Cem. Concr. Compos.* **2021**, *124*, 104240. [[CrossRef](#)]
229. Suraneni, P.; Hajibabae, A.; Ramanathan, S.; Wang, Y.; Weiss, J. New insights from reactivity testing of supplementary cementitious materials. *Cem. Concr. Compos.* **2019**, *103*, 331–338. [[CrossRef](#)]

**Disclaimer/Publisher’s Note:** The statements, opinions and data contained in all publications are solely those of the individual author(s) and contributor(s) and not of MDPI and/or the editor(s). MDPI and/or the editor(s) disclaim responsibility for any injury to people or property resulting from any ideas, methods, instructions or products referred to in the content.